FE-2031-17

FOSSIL ENERGY

CHEMISTRY AND STRUCTURE OF COAL DERIVED ASPHALTENES AND PREASPHALTENES

Quarterly Progress Report for April—June, 1980

By
T. F. Yen

Work Performed Under Contract No. AC01-76ET10626

University of Southern California
School of Engineering
Los Angeles, California

U. S. DEPARTMENT OF ENERGY

DISCLAIMER

DISCLAIMER

Available from the National Technical Information Service, U. S. Department of Commerce, Springfield, Virginia 22161.

Price: Printed Copy A05
Microfiche A01

MAY 18 1981

May 12, 1981

RECEIVED BY TIC MAY 18 1981

Mr. T.W. Laughlin
DOE Technical Information Center
P.O. Box 62
Oakridge, TN 37830

Dear Mr. Laughlin:

Enclosed please find a copy of the erratum for the Fossil Energy report.

Please make copies and distribute them among the people you have sent the report to.

Thank you for your distribution.

Sincerely,

T.F. Yen
Professor
University of Southern California
School of Engineering
Los Angeles, CA 90007

Enclosed:erratum
tfy:hvp

T.F. Yen,
Department of Chemical Engineering
University of Southern California
University Park
Los Angeles, CA 90007

JHS
5/18/81

Erratum to FE-2031-17

"Chemistry and Structure of Coal Derived Asphaltenes and Preasphaltenes"

Quarterly Progress Report for April--June, 1980

By
T.F. Yen

On page 3 after the section on "Objective and Scope of Work", there should have been a footnote as follows:

Note: The material presented in this quaterly report is based on a preliminary copy of Ph.D. dissertation of Mr. Win-Chung Lee entitled "Intercavegim of Coal-Derived Products".

FE-2031-17
Distribution Category UC-90a

CHEMISTRY AND STRUCTURE OF COAL DERIVED ASPHALTENES AND PREASPHALTENES

Quarterly Progress Report for the period
April to June, 1980

University of Southern Calfornia

Contributors

Principle Investigator: T. F. Yen

Research Associates: Wen-Chung Lin
Feng-Fang Shue

Graduate Students: Mankin Chan
Philip Chang
Win-Chung Lee
James Tang
Victoria Weinberg

Major Technical Assistants: Lili Ann Agustin
Eric Arrington
Robert Castenada
Stanley Chen
Lilly Chung

Supporting Students: In Cho
Sandra Chen
Roxanna Manlagnit
Maria Vargas

Prepared for the United States Department of Energy
Under Contract No. EX-76-C-01-2031

OBJECTIVE AND SCOPE OF WORK

It is the objective of this project to isolate the asphaltene and preasphaltene fractions from coal liquids from a number of liquefaction processes. These processes consist of in general: catalytic hydrogenation, staged pyrolysis and solvent refining. These asphaltene fractions may be further separated by both gradient elution through column chromatography, and molecular size distribution through gel permeation chromatography.

Those coal-derived asphaltene and preashpaltene fractions will be investigated by various chemical and physical methods for characterization of their structures. After the parameters are obtained, these parameters will be correlated with the refining and conversion variables which control a given type of liquefaction process. The effects of asphaltene in catalysis, ash or metal removal, desulfurization and denitrification will also be correlated. It is anticipated that understanding the role of asphaltenes in liquefaction processes will enable engineers to both improve existing processes, and to make recommendations for operational changes in planned liquefaction units in the United States.

The objective of Phase 1 was to complete the isolation and separation of coal liquid fractions and to initiate their characterization.

The objective of Phase 2 is to continue the characterization of coal asphaltenes and other coal liquid fractions by use of physical and instrumental methods. The structural parameters obtained will be used to postulate hypothetical average structures for coal liquid fractions.

The objective of Phase 3 is to concentrate on the characterization of the preasphaltene (benzene insoluble fraction) of coal liquid fraction by the available physical and chemical methods to obtain a number of structural parameters.

Interconversion of Coal-Derived Products

A. Description of Experimental Work

1. Separation of Coal Liquid Received

The coal liquid sample received is the so-called "stripper bottom" product from the SRC-II pilot plant operation. The solvent fractionation method of Schwager and Yen[1] has been modified to separate the coal liquid into three fraction: PS, A and BI. The general procedure is shown in Figure 1 and consists of the following steps: the "as received" coal liquid thinned with benzene with a 1:1 ratio of the weight of the coal liquids to the volume of benzene. The mixture is precipitated from a 20-fold (volume to weight) excess of pentane. The precipitate is filtered, washed with pentane, and Soxhlet-extracted until no color is observed in the out-flowing extract. The Soxhlet thimble is then allowed to drain and the pentane insoluble solids air dried. The PS fraction is obtained by removing the pentane from the pentane soluble solution through rotary evaporation. The pentane-insoluble material is Soxhlet-extracted with benzene until the out-flowing extracts are clear. This solution of benzene soluble, but pentane insoluble material is filtered, concentrated by rotary evaporation, and freeze-dried to obtain the A fraction as a power. The Soxhlet thimble is allowed to drain and the benzene-insoluble solids air dried. The trace amount of benzene is the BI fraction is removed in the vacuum oven overnight.

In order to accumulate adequate amounts of each fraction as feedstocks for subsequent experiments, as well as to test the reproducibility of this method, a series of runs were carried out. Corresponding fractions from different runs were mixed thoroughly and contained in glass jars which were carefully stored in a glass desiccator filled with anhydrous calcium chloride as a drying agent, to prevent oxidation by contacting with air.

In everyrun, the starting coal liquid and the three fractions obtained were weighed carefully to get the mass recovery.

The pentane solvent used was a commerical grade, while the benzene was an analytical grade from Mallinckrodt.

2. Autoclave Reaction

A Schematic diagram of the high pressure autoclave system is given in Figure 2 . The autoclave was a conventional 300 ml Magne Drive, stainless steel autoclave made by Autoclave Engineers. It is provided with a liquid sample line a gas sample line, a cooling water line, a thermocouple well, Magne Drive stirrer, pressure gauge, heating jacket, and two extra connections for special uses. A sample injection system was connected through the liquid sample line. All valves and connections were from Swagelok made of 316 stainless steel one quarter inch in size. The tubing and feed vessel (154.5 ml in volume) were also made of stainless steel.

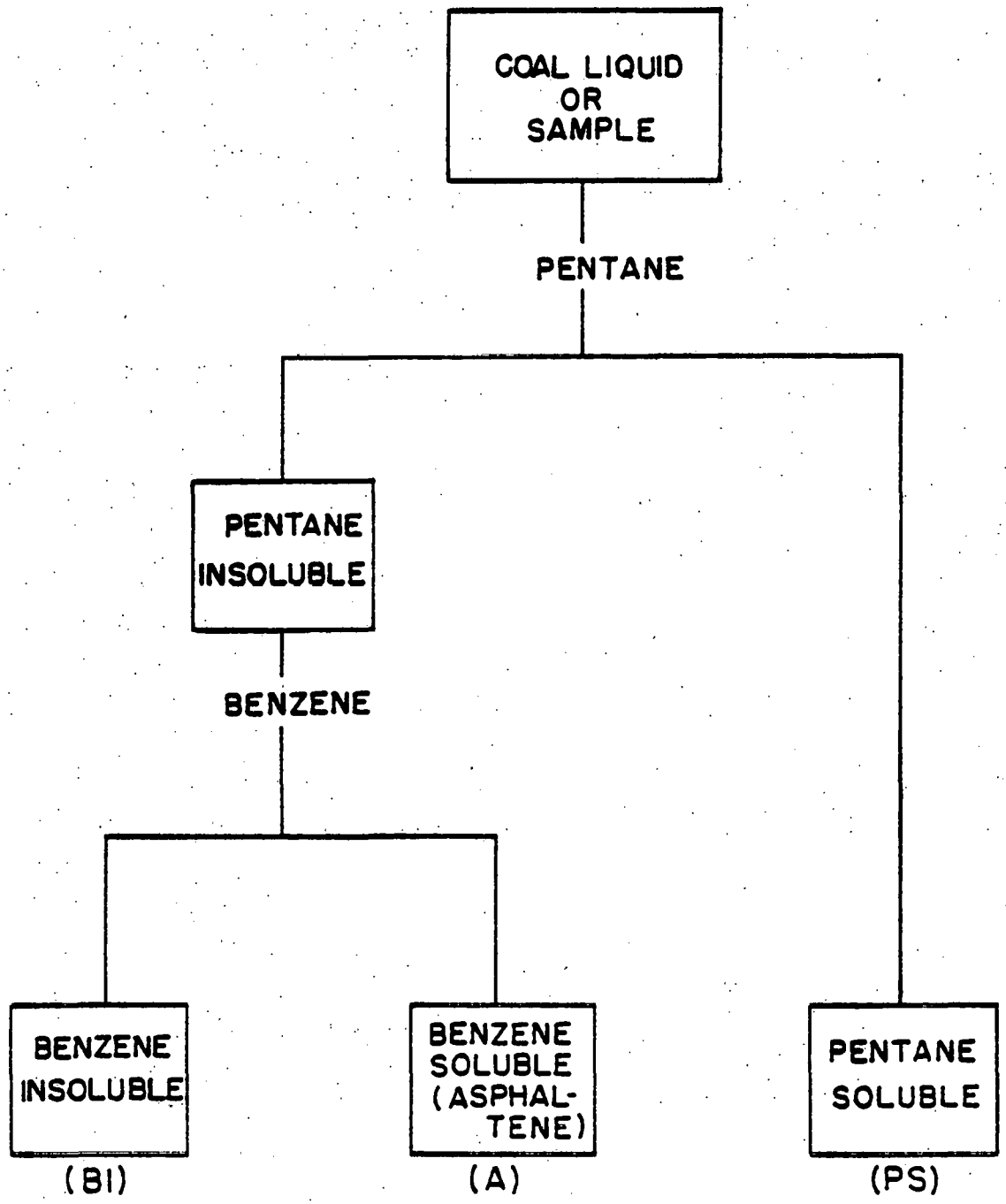

Figure 1. Solvent Fractionation Scheme

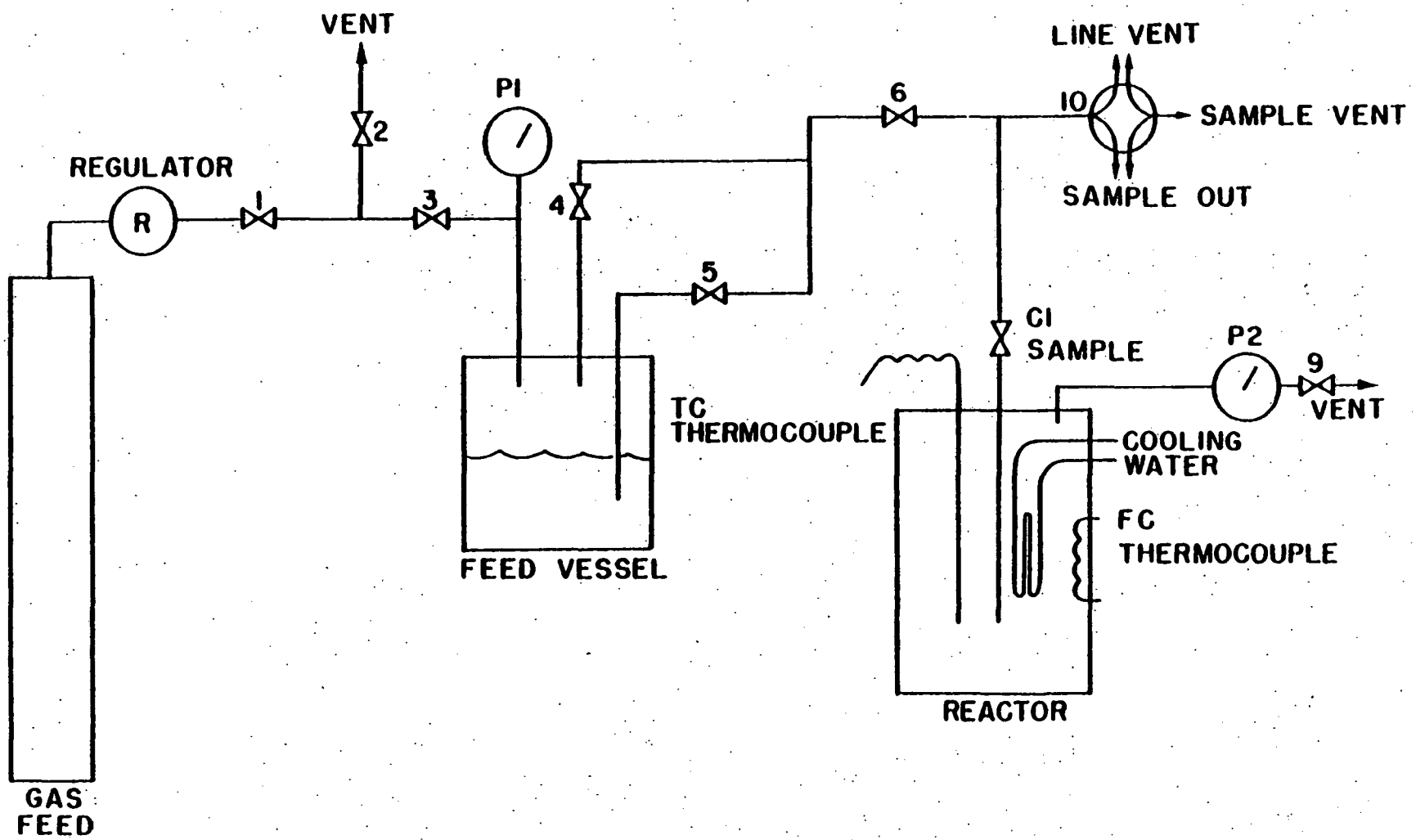

Figure 2. Schematic of Autoclave Reaction System

The temperature is controlled by a temperature controller Model TPD-130-D. It has two thermocouple controls. One is a time proportioning controller with digital readout 0-999° F,which monitors the vessel temperature directly and is the primary controller. A second controller,which is a non-indicating controller,senses the furnace heater temperature and limits it to a safe range. The entire unit is installed in a metal cabinet with suitable power connection and thermocouple connections. The whole system was calibrated before use.

Before an experimental run was started,pure tetralin was charged to the autoclave, while a mixture of sample and tetralin was charged to the feed vessel. The amount of tetralin and mixture,and the ratio of sample to tetralin in the mixture could be varied and was dependent upon the total sample to tetralin ratio. Heating through the heating jacket and stirring in the autoclave were then initiated. After the temperature of the tetralin in the reactor was raised to the desired reaction temperature, the feed vessel containing the mixture was raised to a higher pressure than that in the reactor. By opening the 5,6 and sampling valves,the mixture would be forced into the reactor, and the reaction would begin. At this time,the pressure in the reactor could be adjusted to the desired pressure, and the injection system could be removed. Samples of 5-15 gram each were taken afterward by simply releasing the sampling valve slowly without disturbing the reaction.

The temperature drop after the injection of the mixture from the feed vessel was generally 50-120° F. Recovery to the desired temperature required about 2 minutes, which is negligible compared to the long reaction time.

To complete a run, the electricity to the whole system was shut down and simultaneously cooling water flow was started. The temperature dropped quickly. Usually,cooling lasted overnight to make sure it was completely cool. The product remaining in the reactor and the small amount of mixture remaining in the feed vessel were carefully recovered. All these materials together with samples taken during the reaction were weighed carefully to get the mass recovery.

The pressure in the reactor, after it was completely allowed to cool, did not vary much from the pressure in the feed vessel, by which the mixture was forced into the reactor. This means that the gas production during the reaction is small and may be negligible. An unsuccessful attempt was made to collect the gas by a dry ice trap. Therefore, it was assumed that the gas production was zero.

Analytical grade tetralin solvent was obtained from Fischer Scientific.

3. Separation of Reaction Products

The method that was used to separate the coal liquid has been adopted here to separate the reaction products. The only difference is that the reaction product is precipitated directly from a 20-fold excess of pentane without being thinned with benzene. The pentane soluble fraction actually contains the PS fraction converted from A or BI, and the solvent,which consists of mainly the tetralin as well as the products from tetralin conversion.

4. Characterizations

The first characterization method used in this study is elemental analyses of carbon,hydrogen,nitrogen,sulfur,ash,and oxygen. They were carried out with standard procedures by the ELEK Microanalytical Labs., Torrance, California, and Huffman Labs., Wheatridge, Colorado. Carbon and hydrogen (± 0.3%) were measured by combustion followed by carbon dioxide and water determination; nitrogen (± 0.3%) by the Dumas method; sulfur (± 0.3%) by combustion to sulfur dioxide followed by titration; ash (±0.3%) gravimetrically after combustion at 750°C; and oxygen by difference.

A Mechrolab Model 301A Vapor Pressure Osmometer (VPO) was used to determine molecular weights as a second characterization method. Both the non-aqueous probe and the thermostat were designed for 37° C. Benzil of molecular weight 210.2 was employed as a standard. Since coal-derived products are associated even in dilute solution, the method of extrapolating to infinite dilution to get the true monomer molecular weight, was used.[2-4] In normal runs, 3 or more concentrations over the range 5-30 g/l were employed in the solvent benzene for extrapolation to infinite dilution. A computer program in Fortran IV has been written to calculate the molecular weights from VPO data and to extrapolate the molecular weights at various concentrations to infinite dilution by a least-square fit. (This program is shown in the Appendix as Program 1.)

The proton NMR spectra were run on a varian T-60 spectrometer. The solvent used was 99.8% deuterochloroform plus 1% tetramethylsilane (TMS). TMS is an intenal reference and has absorption at 0.0 ppm. All those solvents were obtained from Marck & Company, Inc. NMR analysis was carried out using modified Brown-Ladner equations.[5] These average structural parameter equations are given in Table I. A program has been written to calculate all those parameters from these equations, as well as molecular formula from molecular weight and elemental analysis. (It is shown in the Appendix as Program 2.) This is the third characterization method.

Table I. Modified Brown-Ladner Equations[a]

$$f_a = \frac{\frac{C}{H} - \frac{H_\alpha}{x} - \frac{H_o}{y}}{\frac{C}{H}} = \text{fraction of total carbon which is aromatic carbon}$$

$$\frac{H_{aru}}{C_{ar}} = \frac{\frac{H_\alpha}{x} + H_{ar} + \frac{O - O_{OH}}{H}}{\frac{C}{H} - \frac{H_\alpha}{x} - \frac{H_o}{y}} = \text{ratio of substitutable aromatic edge atoms to total aromatic atoms}$$

$$\sigma = \frac{\frac{H_\alpha}{x} + \frac{O}{H}}{H_{ar} + \frac{H_\alpha}{x} + \frac{O - O_{OH}}{H}} = \text{fraction of the available aromatic edge atoms occupied by substituents}$$

$$R_s = C_A \frac{H_{aru}}{C_{ar}} = \text{number of substituted aromatic rign carbons}$$

$$n = \frac{H_o}{H_\alpha} + 1 = \text{number of carbon atoms per saturated substituent}$$

$$C_A = \frac{f_a(C)\ (MW)}{100} = \text{total number of aromatic carbon atoms}$$

$$R_A = C_A\left(\frac{1 - H_{aru}/C_{ar}}{2}\right) + 1 = \text{number of aromatic rings}$$

C = mol% carbon H = mol% hydrogen O = mol% oxygen

O_{OH} = mol% phenolic oxygen

H_{ar} = mol fraction aromatic hydrogen

H_α = mol fraction hydrogen α to aromatic ring

H_o = mol fraction of aliphatic hydrogen not α to aryl ring

x = average ratio of hydrogen to carbon on carbons α to aryl ring

y = average ratio of hydrogen to carbon on aliphatic carbons not α to aryl ring

---

[a]Assumptions: All oxygen is attached to aryl rings in ether phenol or aryl ether groups. All phenolic hydrogens found by the TMS derivative method are under the aryl absorption x=y=2.

IR spectra were obtained on a Beckman Acculab 6 instrument. Two sodium chloride cells with 0.1 mm pathlength were used. One cell contained pure solvent and the other contained solution, while the spectrum was taken. The effect of the solvent in this case could be reduced. The base line,i.e., the spectrum obtained with both cells containing pure solvent,was checked very often. This is the fourth method of characterization.

The last characterization method used in this study is the analytical scale high performance liquid chromatography (HPLC). A Waters LC system was used, which was comprised of the following equipment: (1) Waters Associates Model 6000A solvent delivering system, (2) Waters Associates Model 440 absorbance detector 254nm), (3) Waters Associates Model R401 differential refractometer, and (4) Houston Omniscribe 2-pen recorder. Two different kinds of columns were used. The first kind was Micro-Styragel for gel permeation chromatography (GPC), where three columns (two 100 Å and one 500 Å , 7 mm i.d. x 30 cm length, -3,000 plates each) were connected in series, and THF was used as mobile phase solvent. A reverse phase Microbondapak C_{18} (C_{18}) column was the second kind, while a mixture of methanol and water with a volume ratio of 7:3 was used as mobile phase solvent. Before using, all solvent were degassed by sonic bath stirring. Samples were prepared as 3% solutions in THF for GPC, and in methanol for C_{18}. The samples were filtered across a 0.45 micrometer millipore filter before injection. The injection volume was 20 micro-liters, and the flow rate was 1.0 ml/min or 2.0 ml/min. All solvents were glass distilled UV grade. Methanol was obtained from Fischer Scientific, while water and THF were from Burdick and Jackson Laboratories, Inc.

B. Experimental Results

1. Separation of Coal Liquid and Reaction Products

The coal liquid received is a heavy material. It is the bottom product from the flash separator, where about 18% of the light product, mainly naphtha, has been stripped out. The coal liquefaction reaction conditions and the composition of the coal liquid, reported from the Pittsburg and Midway Coal Mining Company, are shown in Table II. The solvent fractionation results of the coal liquid are shown in Table III, where the recovery is defined as the ratio in percentage of the total weight of PS, A and BI obtained after separation to the weight of the starting coal liquid. The coal liquid contains about 48.4% of PS, 15.2% of A, and 36.3% of BI. The recovery by this method is about 98.1%, which indicates a very high yield. So, this method is also used to separate the reaction products. The separation recovery results of those reaction products are shown in Table IV, while the reaction conditions and product distribution will be discussed in the next section. This solvent fractionation analysis became the standard method, and was used throughout this study.

2. Reaction Product Distribution

The calibration curve for the thermocouple of the temperature controller is shown in Figure 3 . Computer-assisted least-squares analysis was carried out for the calibration line. (The program for the least-squares fit is shown in the Appendix as Program 3.) The resulting line, with accompanying standard deviations of the slope and intercept of the line along with correlation coefficient, is also presented in Figure 4 . The constant temperature control of the thermocouple has been tested and shows a $\pm$ 5% variation. For subsequent experiments, the temperature variations were checked often and were within $\pm$5%.

For all reaction experiments, all the reactants and products were weighed out very carefully. The mass recovery for each run is defined as the ratio in percentage of the total weight of products to that of reactants. Table V shows the mass recoveries for all the reaction runs.

The solvent tetralin was used as a hydrogen donor agent in most of the reaction runs. Since it was soluble in pentane, it fell within the PS fraction during the product separation. This fraction is represented by PS + T. The amount of PS was obtained from the following equation based on mass balance:

$$PS = \frac{W}{r + 1} - WA - WBI \qquad (7)$$

Where

Table II. Reaction Conditions and Product Composition of SRC II Stripper Bottom[a]

Sample: SRC II Stripper Bottom

Coal: Pittsburgh Seam Coal, Blackville No. 2 Mine

Temperature: 862° F

Pressure H_2: 1909 psig

Run No.: MBR No. 12[b]

Composition (%):

Naphtha: 0.11 (IBP to 350° F)

Middle Distillate: 0.13 (350 to 550° F)

Heavy Distillate: 43.94 (550 to 850° F)

Vacuum Bottoms: 55.80

% Pyridine Insoluble: 21.50

---

[a]Reported from Pittsburg & Midway Coal Company (PAMCO).

[b]Reaction run number from PAMCO.

Table III. Solvent Fractionation Analysis of SRC II Stripper Bottom

	%Wt.			
	PS	A	BI	%Recovery[a]
	49.9	13.2	36.9	96.7
	47.9	17.6	34.5	99.0
	49.1	17.0	33.9	96.6
	49.4	16.4	34.2	95.8
	47.6	16.3	36.1	97.5
	49.6	15.7	34.7	101.7
	48.5	14.3	37.2	98.9
	48.4	15.0	36.6	99.8
	50.1	15.9	34.0	99.5
	47.6	13.2	39.2	97.3
	47.8	14.6	37.5	99.2
	50.8	14.4	34.9	98.8
	45.5	17.1	37.4	97.8
	48.3	14.3	37.4	97.3
	47.3	14.8	37.9	98.2
	49.0	13.3	37.7	99.2
	47.3	15.0	37.7	96.0
Mean:	48.4	15.2	36.3	98.1
Sd:	1.3	1.3	1.6	1.5

[a]Defined as the ratio of the total weight of PS, A and BI obtained after separation to the weight of coal liquid to be separated.

Table IV. Mass Recovery of Solvent Fractionation Analysis of Reaction Products

Run No.	%Recovery[a]	Run No.	%Recovery[a]	Run No.	%Recovery[a]
2-1	74.4	16	91.2	25-3	97.7
2-2	82.7	17-1	98.0	25-4	97.4
2-3	88.2	17-2	97.1	37-1	88.9
2-4	94.0	17-3	96.9	37-2	94.0
2-6	95.9	17-4	96.0	37-3	96.1
2-7	97.5	17-5	96.7	37-4	93.5
2-8	100.4	18-1	97.4	37-5	96.5
5	94.3	18-2	97.0	37-6	83.8
7	97.4	18-3	99.9	37-7	97.6
8	94.2	19-1	96.0	38-1	95.8
9	97.3	19-2	94.7	38-2	95.1
13-3	96.7	19-3	96.3	38-3	89.5
14-1	95.9	19-4	94.0	38-4	95.1
14-2	96.4	24-1	93.8	38-5	93.4
15-1	83.8	24-2	95.5	38-7	103.8
15-2	96.6	24-3	94.4	39-1	93.8
15-3	97.7	25-1	94.1	39-2	91.3
15-4	99.1	25-2	95.0	39-3	83.3
(Continued to next column)		(Continued to next column)			

Mean: 94.3 Standard Deviation: 5.0

[a] Defined as the ratio of the total weight of all fractions obtained after separation to the weight of the product to be separated.

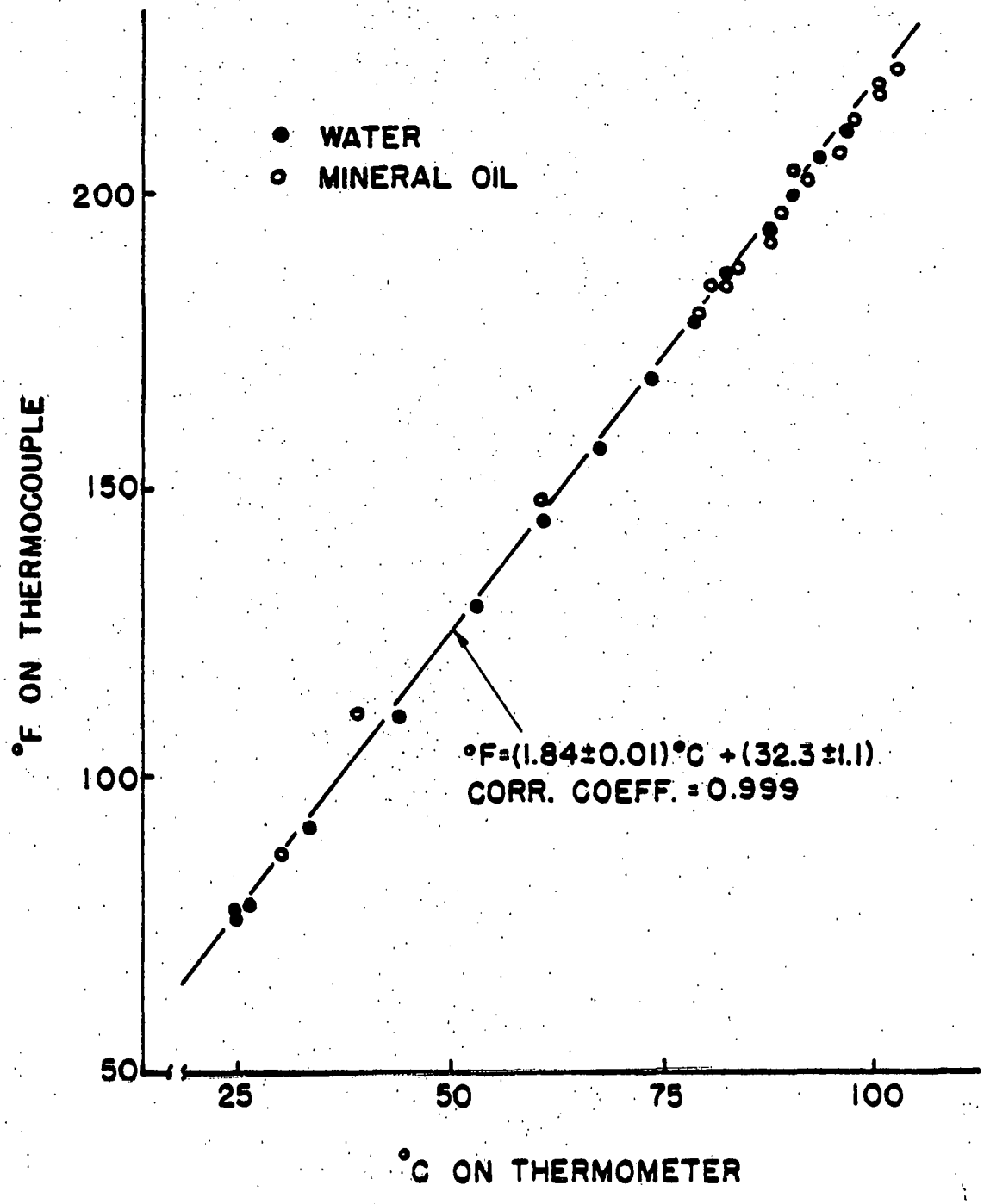

Figure 4. Calibration Curve for the Thermocouple of the Temperature Controller

Table V. Mass Recovery[a] of Reaction Runs

Run No.	Reaction Conditions: Reactant	Temp. (°F)	Pre. (psi)	TTR[b] Ratio	Total Weight: Reactant (gram)	Tetralin (gram)	Product (gram)	Mass[a] Recovery (%)
2	PS	650	800	2:1	70.00	140.00	191.69	91.3
3	A	650	1800	5:1	33.45	167.25	182.40	90.9
5	A	760	1800	5:1	33.30	166.70	154.70	77.4
7	PS	750	800	5:1	20.00	100.00	116.20	96.8
8	PS	800	1900	5:1	20.00	100.50	114.60	95.1
9	BI	800	1800	5:1	20.00	100.00	110.60	92.0
13	A	705	800	5:1	20.00	99.90	116.10	96.8
14	A	705	800	5:1	20.00	99.90	116.60	97.2
15	A	705	800	5:1	20.00	100.00	114.50	95.4
16	PS	705	800	0	80.00	0.00	58.70	73.4
17	A	760	800	5:1	19.50	100.00	116.23	97.2
18	A	760	800	5:1	20.00	99.60	110.86	92.7
19	A	760	800	5:1	20.00	99.50	127.36	106.6
24	A	705	800	5:1	20.00	100.00	88.25	73.5
25	A	705	800	5:1	20.00	100.00	113.30	94.4
37	A	820	800	5:1	25.00	125.00	124.73	83.2
38	A	820	800	5:1	25.00	125.00	126.76	84.5
39	A	705	800	5:1	20.00	100.00	106.96	89.1

Mean Mass Recovery: 90.4 Standard Deviation: 8.6

[a]Defined as the ratio of the total weight of all products to the total weight of all reactants and tetralin.

[b]Tetralin to reactant ratio.

W: amount of the product to be separated
r: tetralin to reactant ratio
WA: amount of asphaltene obtained after separation
WBI: amount of benzene insoluble fraction obtained after separation

Vacuum distillation was used to separate the PS fraction and tetralin, and the result was very close to that obtained from the above equation. So, Equation (7) has been used to calculate the amount of PS fraction throughout this study.

The conversion results of all reaction experiments, together with the reaction conditions, are shown in Tables VI to XI. Table VI shows the reaction results of the PS fraction at various conditions, while the isothermal reaction results are shown in Table VII. The results show that, with tetralin as a vehicle oil, only small or negligible amounts of PS are converted into A and BI fractions.

Table VIII shows the conversion results on the A and BI fractions. It indicated that 40 to 70 percent of the A has been converted to PS or BI, and the PS fraction was also formed from the BI fraction. All runs in this table were carried out in the early stages of this study, and the sample injection system was not used during those runs. Sample and solvent were sealed in the reactor, which was heated up to the reaction temperature and maintained for the desired period. After the reactor was completely cool, the product was taken out and analyzed.

In order to get conversion data for the kinetic study, a series of experiments was carried out very carefully, using the injection system described previously to eliminate the time for warm up and cool down. Tables IX to XI show the results from isothermal conversions of the A fraction at 705° ,760° and 820°F, respectively. The product distributions vs. time of the above isothermal reactions are shown in Figures 5, 6 amd 7. where the weight percentage of the PS is represented by solid dots, those of A by triangles, and those of BI by open circles.

3. Kinetic Model of Interconversion of Coal-Derived Products

From the above results, the reaction scheme for the isothermal conversion can be best rationalized as follows among a few others which have been tested, and its validation will be seen in Chapter 6.2:

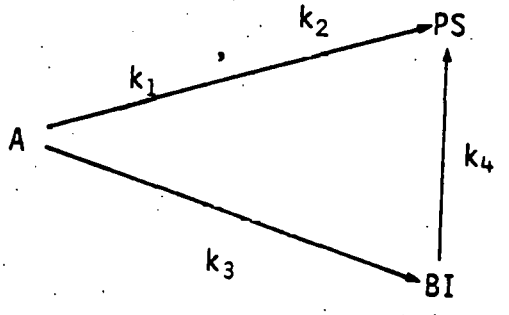

where

k_1: rate constant of primary decompostition reaction of A
k_2: rate constant of secondary decomposition reaction of A
k_3: rate constant of polymerization reaction of A
k_4: rate constant of decomposition reaction of BI

Table VI. Conversion Results on SRC II-PS

Run No.	Reaction Conditions				Product Distribution (%Wt.)		
	Temp. (°F)	Pre. (psi)	Time (hr)	Tetralin to PS Ratio	PS	A	BI
7	750	800	24	5:1	99.0	<1.0	<0.1
8	800	1900	24	5:1	99.0	<1.0	<0.1
2-8	650	800	24	2:1	93.8	6.0	0.2
16	705	800	2	0	73.4	22.8	3.8

Table VII. Isothermal Reaction Results on SRC II-PS at 650° F

(Pressure: 800 psi Tetralin to PS Ratio: 2:1)

Run No.	Time (hr)	Product Distribution (%Wt.) PS	A	BI
2-1	0.5	97.0	1.2	1.8
2-2	1.0	95.4	1.8	2.8
2-3	2.0	92.6	4.6	2.9
2-4	3.0	94.4	4.1	1.5
2-6	5.0	96.0	2.5	1.5
2-7	24.0	95.2	3.5	1.3

Table VIII. Conversion Results on SRC II-A and BI

(Tetralin to Sample Ratio: 5:1)

Run No.	Sample	Experimental Conditions Temp. (°F)	Pre. (psi)	Time (hr)	Product Distribution (%Wt.) PS	A	BI
3	A	650	1800	24	42.1	38.5	19.5
13-3	A	705	800	24	48.9	35.8	15.3
5	A	760	1800	24	69.8	30.2	0.1
9	BI	800	1800	17	7.3	4.8	87.9

Table IX. Isothermal Reaction Results on SRC II-Asphaltene at 705° F, 800 psig of N_2

(Tetralin to Asphaltene Ratio: 5:1)

Run No.	Time (hr)	Product Distribution (%Wt.)		
		PS	A	BI
24-1	0.25	35.3	48.3	16.4
14-1	0.50	46.6	44.1	9.3
24-2	0.50	47.8	37.1	15.2
14-2	1.0	34.2	59.9	5.9
24-3	1.0	46.9	41.4	11.7
15-1	2.0	30.8	54.8	14.3
25-1	2.0	49.2	43.0	7.8
15-2	3.0	40.0	56.1	3.9
15-3	4.0	35.9	60.8	3.4
25-2	4.0	32.3	56.1	11.6
39-1	4.0	34.1	54.3	11.6
15-4	5.0	36.6	61.3	2.1
25-3	5.0	49.0	40.4	10.6
25-4	7.0	64.8	30.2	5.0
39-2	9.0	45.9	54.0	0.1
39-3	17.0	72.4	26.5	1.1

Table X. Isothermal Reaction Results on SRC II-Asphaltene at 760° F, 800 psig of N_2

(Tetralin to Asphaltene Ratio: 5:1)

Run No.	Time (hr)	Product Distribution (%Wt.) PS	A	BI
17-1	0.25	49.3	44.2	6.4
17-2	0.50	51.5	42.5	6.0
17-3	0.75	49.1	43.9	7.0
17-4	1.00	48.2	44.9	6.9
17-5	1.50	48.1	44.7	7.1
18-1	1.50	49.9	42.8	7.3
18-2	2.00	48.1	43.6	8.3
18-3	3.00	52.2	43.9	3.9
19-1	5.00	73.0	24.5	2.6
19-2	7.00	77.1	21.6	1.3
19-3	10.00	77.2	18.9	3.8
19-4	22.00	85.7	12.6	1.7

Table XI. Isothermal Reaction Results on SRC II-Asphaltene at 820^{o} F, 800 psig of N_2

(Tetralin to Asphaltene Ratio: 5:1)

Run No.	Time (hr)	Product Distribution (%Wt.) PS	A	BI
37-1	0.25	25.8	71.7	2.5
38-1	0.25	28.1	64.9	7.0
37-2	0.50	29.3	58.7	12.0
37-3	0.75	34.1	52.3	13.6
37-4	1.50	26.7	63.8	9.5
38-2	1.50	38.8	57.1	4.1
37-5	2.00	35.6	54.9	9.6
37-6	3.00	24.4	73.6	2.0
37-7	4.00	47.8	48.5	3.7
38-3	6.00	49.6	48.6	1.8
38-4	9.00	58.7	40.8	0.5
38-5	13.00	53.7	45.2	1.1
38-6	18.00	38.0	49.5	12.5
38-7	24.00	74.9	24.8	0.4

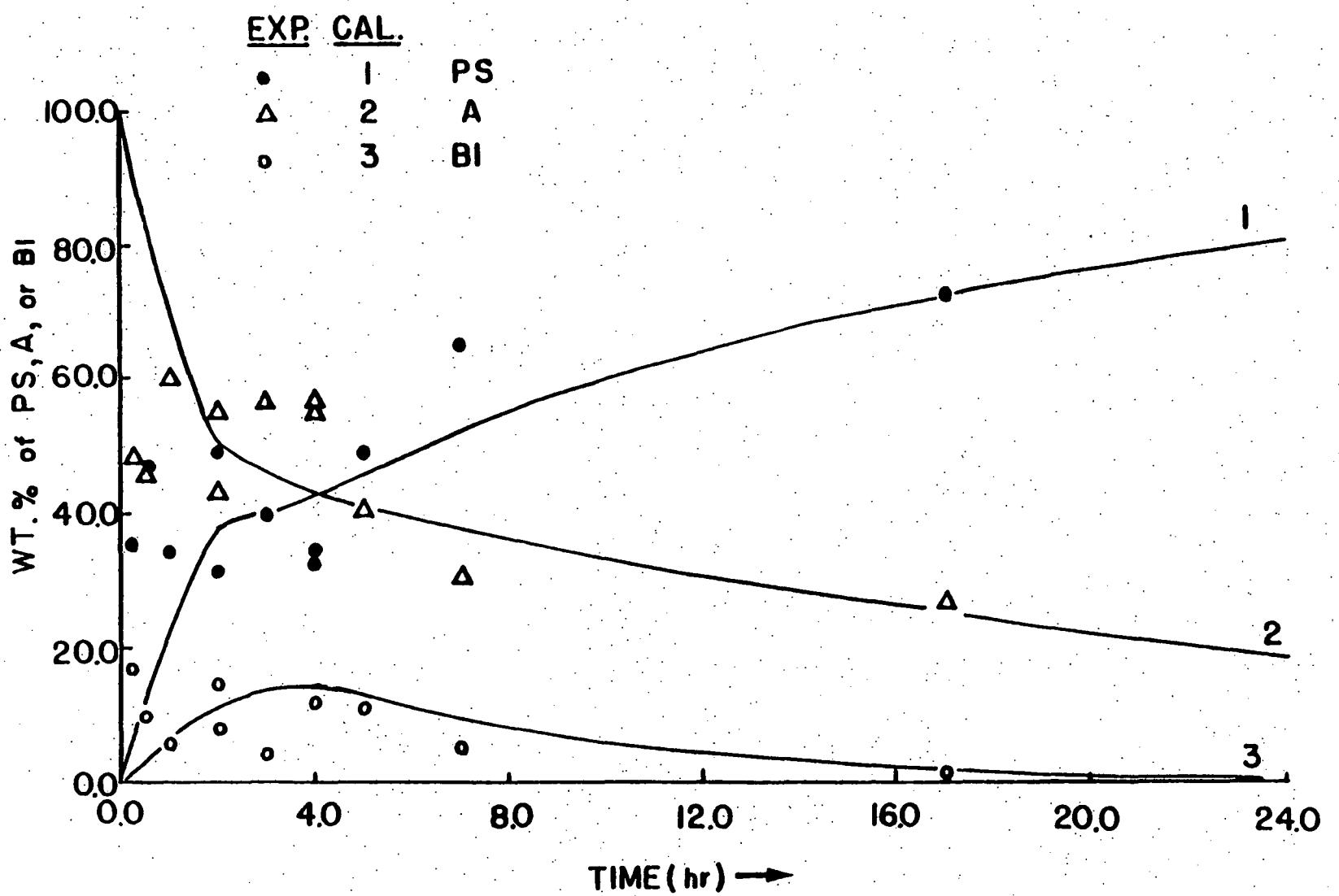

Figure 5. Product Distribution of Isothermal Reaction on SRC II-A at 705° F, 800 psig of N_2 (Experimental Data and Model Prediction)

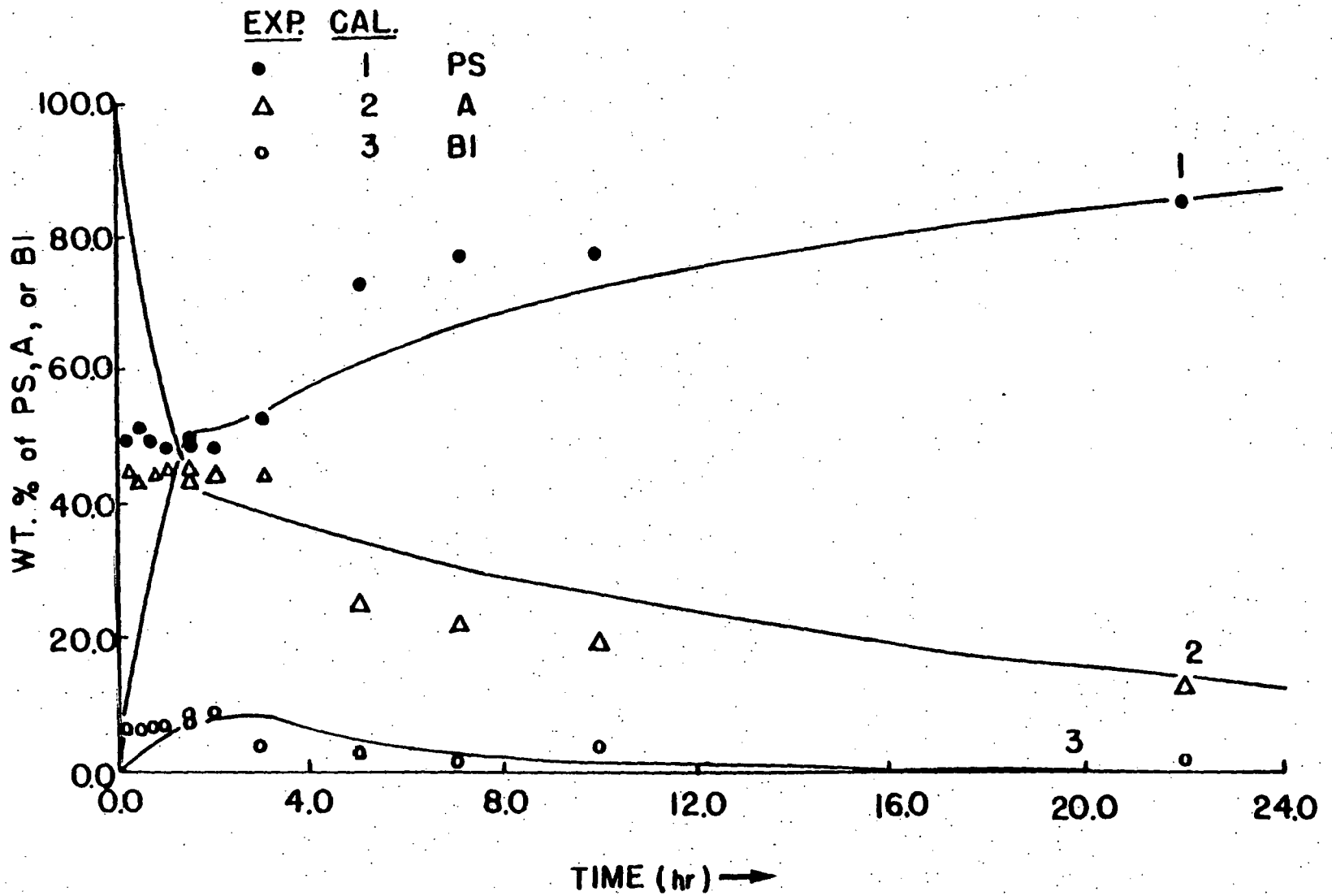

Figure 6. Product Distribution of Isothermal Reaction on SRC II-A at 760°F, 800 psig of N_2 (Experimental Data and Model Prediction)

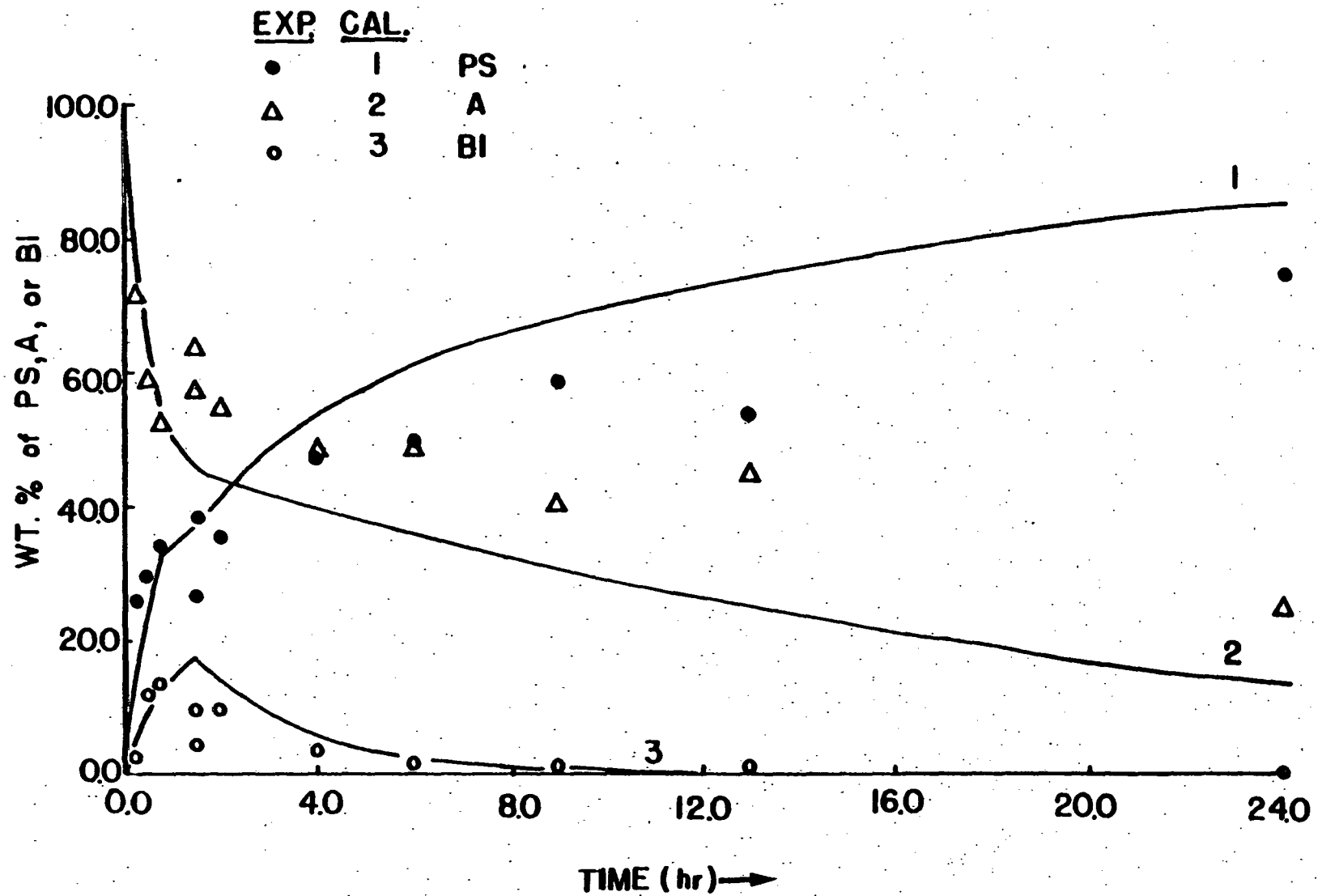

Figure 7. Product Distribution of Isothermal Reaction on SRC II-A at 820° F, 800 psig of N_2 (Experimental Data and Model Prediction)

From (i), it is clear that the A can be converted into PS and BI through two parallel reaction routes by a decomposition reaction accompanied with a polymerization reaction. In this study, decomposition is faster than the polymerization. The formation of BI by polymerization of A reaches a maximum, then the decomposition reaction directly to PS begins. It is followed by the further decomposition of A into PS. Due to the presence of tetralin, the PS fraction formed in the first stage does not polymerize In the later stage of the conversion reaciton.

According to the reaction time (t), specifically, the above-mentioned reaction scheme can be divided into three stages.

The first stage contains mainly the conversion of the A into PS and BI through two parallel reaction routes. This reaction starts right after the sample is injected into the reactor and ends when the t is t_1. It can be represented by

$0 < t \leq t_1$

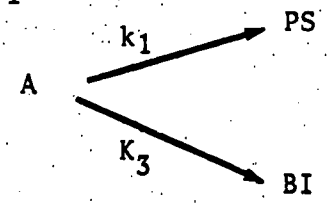

(ii)

The following differential equations represent the rate of disappearance and formation of reactant and products for this model

$$\frac{dA}{dt} = -(k_1 + K_3)\, A \qquad (8)$$

$$\frac{dPS}{dt} = k_1 \cdot A \qquad (9)$$

$$\frac{dBI}{dt} = k_3 \cdot A \qquad (10)$$

Initial conditions using weight fractions are: at t=0, A=100, PS = BI =0.

In the second stage the polymerization reaction of A to BI continues, while the decomposition reaction of BI to PS begins. It can be represented by $t_1 < t \leq t_2$

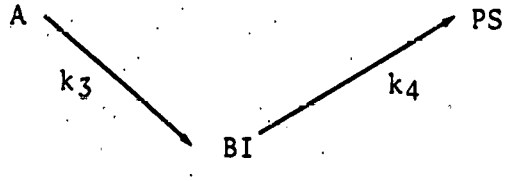

(iii)

The rates of formation and disappearance are then given by

$$\frac{dA}{dt} = - k_3 \cdot A \qquad (11)$$

$$\frac{dBI}{dt} = k_3 . A - k_4 \cdot BI \qquad (12)$$

$$\frac{dPS}{dt} = k_4 \cdot BI \qquad (13)$$

Initial conditions are: at $t=t_1$, $A=A_1$, $PS=PSt_1$, $BI=BIt_1$, where At_1, PSt_1, BIt_1, are the weight fractions of A, PS and BI, respectively obtained from the last stage when $t=t_1$.

When the secondary decomposition reaction of A begins, the third stage starts. The decomposition reaction of BI into PS continues during this period. The reaction scheme for this section is $t_2 < t$

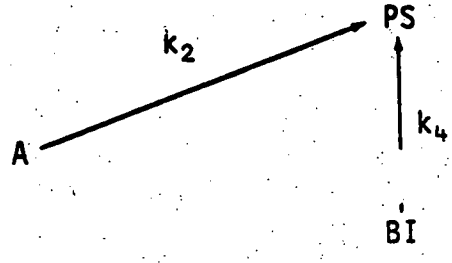

(iv)

The rates of formation and disappearance are then given by

$$\frac{dA}{dt} = - k_2 \cdot A \qquad (14)$$

$$\frac{dPS}{dt} = k_2 \cdot A + k_4 \cdot BI \qquad (15)$$

$$\frac{dBI}{dt} = - k_4 \cdot BI \qquad (16)$$

Initial conditions are at $t=t_2$, $A=At_2$, $PS=PSt_2$, $BI=BIt_2$, where At_2, PSt_2, BIt_2 are the weight fractions of A, PS and BI respectively, obtained from the second section when $t=t_2$.

In all stages, first order kinetics are assumed. The analytical solutions of the differential equations for each section can be obtained and are shown as follows:

$0 < t \leq t_1$

$$A = 100 \cdot \exp\left[-(k_1 + k_3) \cdot t\right] \tag{17}$$

$$PS = 100 \cdot \left[k_1/(k_1 + k_3)\right] \cdot \left\{1 - \exp\left[-(k_1 + k_3) \cdot t\right]\right\} \tag{18}$$

$$BI = 100 \cdot \left[k_3/(k_1 + k_3)\right] \cdot \left\{1 - \exp\left[-(k_1 + k_3) \cdot t\right]\right\} \tag{19}$$

$t_1 < t \leq t_2$

$$A = At_1 \cdot \exp\left[-k_3 \cdot (t - t_1)\right] \tag{20}$$

$$\begin{aligned} PS = {} & PSt_1 - k_4 \cdot At_1 \cdot \left\{\exp\left[-k_3 \cdot (t - t_1)\right] - 1.\right\}/(k_4 - k_3) \\ & - \left\{BIt_1 - k_3 \cdot At_1/(k_4 - k_3)\right\} \cdot \left\{\exp\left[-k_4 \cdot (t - t_1)\right] - 1.\right\} \end{aligned} \tag{21}$$

$$\begin{aligned} BI = {} & At_1 \cdot k_3 \cdot \left\{\exp\left[-k_3 \cdot (t - t_1)\right] - \exp\left[-k_4 \cdot (t - t_1)\right\}/(k_4 - k_3)\right. \\ & + BIt_1 \cdot \exp\left[-k_4 \cdot (t - t_1)\right] \end{aligned} \tag{22}$$

$t_2 < t$

$$A = At_2 \cdot \exp\left[-k_2 \cdot (t - t_2)\right] \tag{23}$$

$$\begin{aligned} PS = {} & PSt_2 + At_2 \cdot \left\{1 - \exp\left[-k_2 \cdot (t - t_2)\right]\right\} \\ & + BIt_2 \cdot \left\{1 - \exp\left[-k_4 \cdot (t - t_2)\right]\right\} \end{aligned} \tag{24}$$

$$BI = BIt_2 \cdot \exp\left[-k_4 \cdot (t - t_2)\right] \tag{25}$$

4. Analytical Characterization of Reactants and Products

The elemental analyses of the SRC II solvent fractions and asphaltenes from various reaction products are given in Tables XII to XV, along with the VPO molecular weights of those samples at infinite dilution. The molecular weights of various samples from VPO determination vs. solvent concentration in g/l are shown in Tables XVI to XIX. Computer-assisted least-squares lines, with accompanying standard deviations of the slopes and intercepts of the lines along with correlation coefficients, are included.

The elemental analysis is reported in percentage, while the concentration is in g/l. The samples A3, A5 and A16 are the asphaltenes isolated from the reaction products of Run Nos. 3,5, 13-3 and 16, respectively, by the standard solvent fractionation analysis. Benzene was used as a solvent for most of VPO determination, while tetrahydrofuran (THF) was also used for some cases. Only the molecular weights of 43,45 and A19-3 are reported at finite concentration, the rest are reported at infinite dilution.

As an example, the proton NMR spectrum of SRC II asphaltene is shown in Fig. 8. Brown-Ladner analysis requires that the three areas of absorption centered at δ= 7.3,2.4 and 1.2 ppm be assigned respectively to aromatic ring hydrogens (H_{ar}), aliphatic hydrogens adjacent to aromatic ring (H_α), and aliphatic hydrogens not adjacent to aromatic rings (H_o). The separation point between the H_α and H_o protons was chosen at δ= 1.73 ppm.[26]

If 90% of oxygen is assumed phenolic, the maximum variation of the properties obtained with or without this correction is within 4%. Therefore, no attempt has been made to determine the phenolic oxygen. The average molar properties of PS, A, A5 and asphaltenes after isothermal reaction at 705°, 760° and 820°F, thus obtained, are presented in Tables XX to XXIII. The molecular formulae of these samples are shown in Table XXIV.

Assignments for the various peaks in the infrared region are well established from earlier works,[6-7] and are shown in Figure9 for the PS fraction. For comparison, IR spectra of three PS + T fractions from isothermal reaction products are also shown. The reaction time is one hour for these three products. IR spectra of the PS fractions from rest products are quite similar to these three and therefore not shown.

The GPC chromatogram of the SRC II-A is shown in comparison with some of the asphaltenes after reaction in Fig. 10. The result of SRC II-PS is also shown in comparison with some of the PS reaction products in Fig. 11. These products contain PS fractions converted from A and tetralin solvent.

Table XII. Ultimate Analysis (%) and Molecular Weight of SRC II Fractions

Sample	C	H	O[a]	N	S	Ash	MW[b]	H/C[c]
PS	90.34	7.44	0.26	1.51	0.40	0.05	192.9	0.99
A	89.31	5.81	2.11	2.00	0.45	0.32	358.0	0.78
BI	60.39	3.05	——	0.84	4.54	31.58		
TS	86.08	5.08	2.59	5.98	2.11	0.16		0.71
TI	57.18	2.55	2.89	0.91	1.18	35.29		0.54
A5	90.42	5.73	1.28	1.79	0.28	0.50	385.1[d]	0.76

[a]By difference.

[b]Molecular weight averaged at infinite dilution in benzene and in THF.

[c]Atomic ratio of hydrogen to carbon.

[d]Molecular wight at 10.3 g/l in THF.

Table XIII. Ultimate Analysis (%) and Molecular Weight of Asphaltenes after Isothermal Reaction at 705° F

Sample	C	H	O[a]	N	S	Ash	MW[b]	H/C[c]
24-1	87.77	5.74	2.61	2.11	0.79	0.98	375.9	0.78
14-2	87.44	5.53	2.88	2.14	0.44	1.57	472.1	0.75
24-3	89.24	5.63	2.39	2.10	0.54	<0.10	359.3	0.75
25-1	88.57	5.64	2.28	2.15	0.86	0.50	379.2	0.76
15-3	87.83	5.44	3.14	2.22	0.72	0.65	447.1	0.74
15-4	85.10	5.75	3.99	1.91	0.39	2.86	511.2	0.80
25-4	87.96	5.66	3.38	2.25	0.66	0.09	383.9	0.77

[a]By difference.

[b]Molecular weight at infinite dilution in benzene.

[c]Atomic ratio of hydrogen to carbon.

Table XIV. Ultimate Analysis (%) and Molecular Weight of Asphaltenes after Isothermal Reaction at 760° F

Sample	C	H	O[a]	N	S	Ash	MW[b]	H/C[c]
17-1	86.85	5.49	4.08	1.98	0.49	1.11	454.5	0.75
17-4	87.09	5.49	4.28	2.23	0.46	0.45	389.6	0.75
17-5	87.36	5.42	4.47	2.20	0.45	<0.10	413.7	0.74
18-2	88.84	5.41	2.21	2.09	0.59	0.86	390.1	0.73
18-3	88.16	5.55	3.38	2.06	0.84	0.01	426.0	0.75
19-1	89.13	5.47	2.20	2.11	1.05	0.04	378.0	0.73
19-3	88.94	5.47	2.32	2.12	0.82	0.33	477.4[d]	0.73

[a]By difference.

[b]Molecular weight at infinite dilution in benzene.

[c]Atomic ratio of hydrogen to carbon.

[d]Average molecular weight at 6.28 g/l in benzene.

Table XV. Ultimate Analysis (%) and Molecular Weight of Asphaltenes after Isothermal Reaction at 820° F

Sample	C	H	O[a]	N	S	Ash	MW[b]	H/C[c]
38-1	87.82	5.71	3.47	2.16	0.74	<0.10	361.9	0.77
37-2	87.48	5.70	3.78	2.12	0.76	0.16	346.0	0.77
37-3	87.65	5.66	3.63	2.05	0.42	0.59	374.3	0.77
37-4	88.05	5.69	3.24	2.06	0.67	0.29	371.6	0.77
37-5	87.90	5.44	3.58	2.03	0.68	0.37	375.2	0.74
37-7	88.74	5.43	3.02	2.28	0.45	0.08	343.6	0.73
38-3	85.49	5.78	6.27	2.00	0.42	0.04	368.2	0.80
38-4	87.29	5.32	4.29	2.11	0.89	0.10	325.8	0.73
38-7	89.10	5.44	3.24	1.86	0.26	0.10	297.9	0.73

[a]By difference.

[b]Molecular weight at infinite dilution in benzene.

[c]Atomic ratio of hydrogen to carbon.

Table XVI. Molecular Weight of SRC II-Fractions and Asphaltenes from Reaction Products vs. Concentration in THF and Benzene

Sample	Solvent	Least Squares Equation[a]	Standard Deviation MW	Slope	Intercept	Corr. Coeff.	MW at Infinite Dilution
PS	THF	MW = 0.55·C + 193.20	2.28	0.08	1.51	0.92	193.2
	Benzene	MW = 0.37·C + 192.54	3.07	0.04	1.22	0.90	192.5
A	THF	MW = 1.29·C + 376.12	10.68	0.16	5.02	0.88	376.1
	Benzene	MW = 3.17·C + 340.35	8.78	0.10	3.48	0.99	340.4
A3	THF	(Concentration: 6.96 g/l)					393.4
A5	THF	(Concentration: 10.3 g/l)					385.1
A13-3	THF	MW = 1.43·C + 403.84	5.57	0.33	5.14	0.87	403.8
A16	THF	MW = 2.04·C + 354.20	8.96	0.49	7.34	0.84	352.4

[a]Molecular weight vs. concentration (in g/l).

Table XVII. Molecular Weight of Asphaltenes after Isothermal Reaction at 705° F, vs. Concentration in Benzene

Sample	Least Squares Equation[a]	Standard Deviation			Corr. Coeff.	MW at Infinite Dilution
		MW	Slope	Intercept		
24-1	MW = 6.18·C + 375.91	11.04	0.56	9.59	0.98	375.9
14-2	MW = 5.20·C + 472.06	15.34	0.94	14.51	0.94	472.1
24-3	MW = 5.49·C + 359.25	9.22	0.60	9.29	0.98	359.2
25-1	MW = 7.59·C + 379.15	4.10	0.24	3.65	0.998	379.2
15-3	MW = 9.49·C + 447.13	4.94	0.22	3.64	0.998	447.1
15-4	MW = 7.67·C + 511.23	13.18	0.63	10.60	0.98	511.2
25-4	MW = 8.18·C + 383.89	3.12	0.18	2.90	0.999	383.9

[a]Molecular weight vs. concentration (in g/l).

Table XVIII. Molecular Weight of Asphaltenes after Isothermal Reaction at 760° F, vs. Concentration in Benzene

Sample	Least Squares Equation[a]	Standard Deviation MW	Slope	Intercept	Corr. Coeff.	MW at Infinite Dilution
17-1	MW = 7.76·C + 454.52	3.16	0.53	6.24	0.99	454.5
17-4	MW = 9.36·C + 389.60	10.98	0.59	9.45	0.99	389.6
17-5	MW = 6.91·C + 413.69	5.89	0.36	6.18	0.99	413.7
18-2	MW = 8.80·C + 390.07	2.27	0.14	2.18	0.999	390.1
18-3	MW = 5.52·C + 426.02	2.63	0.14	2.30	0.998	426.0
19-1	MW = 8.99·C + 377.96	9.42	0.57	8.40	0.99	378.0
19-3	483.63 475.36 at 6.28 g/l 473.04	Average: 477.35			% Deviation: 1.32	

[a]Molecular weight vs. concentration (in g/l).

Table XIX. Molecular Weight of Asphaltenes after Isothermal Reaction at 820° F, vs. Concentration in Benzene

Sample	Least Squares Equation[a]	Standard Deviation			Corr. Coeff.	MW at Infinite Dilution
		MW	Slope	Intercept		
38-1	Mw = 4.99·C + 361.88	0.73	0.04	0.63	0.999	361.9
37-2	MW = 4.43·C + 346.01	8.26	0.39	6.91	0.984	346.0
37-3	MW = 5.58·C + 374.33	1.28	0.05	1.06	0.999	374.3
37-4	MW = 5.59·C + 371.55	3.91	0.17	3.33	0.997	371.6
37-5	MW = 4.26·C + 375.19	3.59	0.22	3.30	0.994	375.1
37-7	MW = 6.42·C + 343.60	2.88	0.16	2.26	0.998	343.6
38-3	MW = 6.18·C + 368.22	1.25	0.09	1.51	0.999	368.2
38-4	MW =11.11·C + 325.78	7.85	0.53	7.48	0.995	325.8
38-7	MW = 4.21·C + 297.89	0.50	0.04	0.76	0.999	297.9

[a]Molecular weight vs. concentration (in g/l).

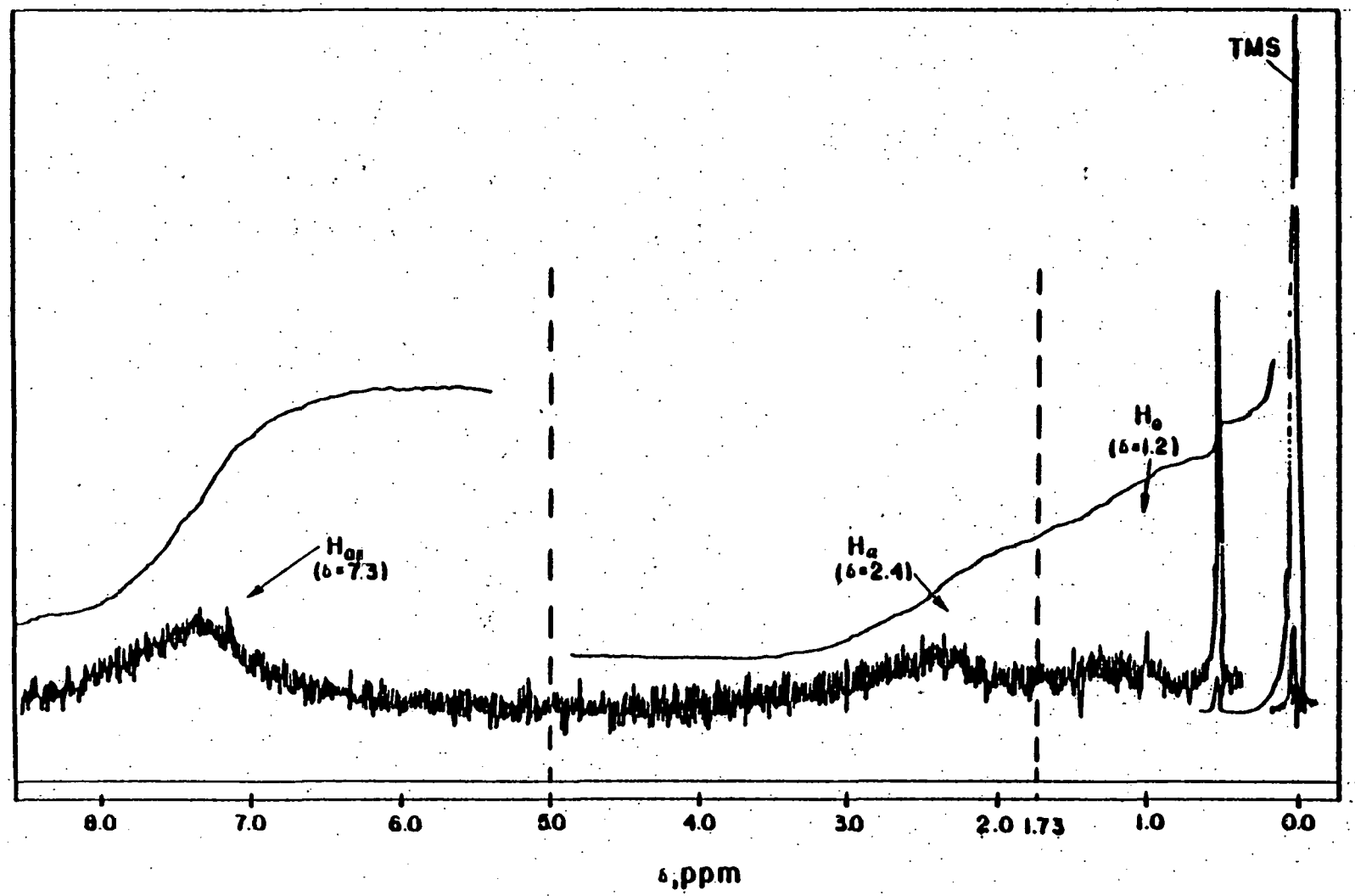

Figure 8. Proton NMR Spectrum of SRC II Asphaltene

Table XX. Average Molar Properties[a] of PS, A, and A5

Average[a] Molar Properties	PS	A	A5
Molecular Formula	$C_{14.52}H_{14.24}N_{0.21}O_{0.03}S_{0.02}$	$C_{26.71}H_{20.70}N_{0.51}O_{0.47}S_{0.05}$	$C_{29.14}H_{22.00}N_{0.49}O_{0.31}S_{0.03}$
H_{ar}	47.2	52.94	55.34
H_{α}	35.2	28.0	25.64
H_{o}	17.6	19.06	19.03
f_a	0.74	0.82	0.83
H_{aru}/C_{ar}	0.86	0.66	0.63
σ	0.27	0.24	0.20
R_s	2.54	3.38	3.13
n	1.50	1.68	1.74
C_A	10.77	21.85	24.24
R_A	1.75	4.75	5.46

[a]See Table I for definition.

Table XXI. Average Molar Properties[a] of Asphaltenes after Isothermal Reaction at 705° F

Average[a] Molar Properties	24-1	14-2	24-3	25-1	15-3	15-4	25-4
H_{ar}	55.6	57.3	59.1	53.6	61.7	59.6	58.4
H_{α}	31.0	29.4	29.4	31.3	25.5	25.3	28.6
H_{o}	13.4	13.4	11.5	15.1	12.8	15.1	13.0
f_a	0.83	0.84	0.85	0.82	0.86	0.84	0.84
H_{aru}/C_{ar}	0.70	0.68	0.68	0.66	0.67	0.74	0.70
σ	0.25	0.24	0.23	0.25	0.21	0.22	0.24
R_s	3.97	4.74	3.49	3.88	3.98	5.12	3.90
n	1.43	1.45	1.39	1.48	1.50	1.59	1.45
C_A	22.97	29.31	22.64	23.18	28.29	31.25	23.67
R_A	4.48	5.74	4.63	4.93	5.65	5.10	4.58

[a]See Table I for definition.

Table XXII. Average Molar Properties[a] of Asphaltenes after Isothermal Reaction at 760° F

Average[a] Molar Properties	17-1	17-4	17-5	18-2	18-3	19-1	19-3
H_{ar}	58.2	59.0	55.1	59.5	61.8	52.4	57.5
H_{α}	28.5	26.3	33.2	27.8	26.0	33.4	33.7
H_{o}	13.2	14.7	11.7	12.7	12.2	14.2	8.8
f_a	0.84	0.85	0.83	0.85	0.86	0.83	0.84
H_{aru}/C_{ar}	0.69	0.68	0.68	0.65	0.69	0.63	0.67
σ	0.25	0.23	0.28	0.22	0.21	0.27	0.25
R_s	4.74	3.86	4.85	3.49	3.95	3.95	5.08
n	1.46	1.56	1.35	1.45	1.47	1.42	1.26
C_A	28.04	24.03	25.15	24.85	26.82	23.20	29.96
R_A	5.35	4.79	5.00	5.39	5.18	5.24	5.97

[a]See Table I for definition.

Table XXIII. Average Molar Properties[a] of Asphaltenes after Isothermal Reaction at 820° F

Average[a] Molar Properties	38-1	37-2	37-3	37-4	37-5	37-7	38-3	38-4	38-7
H_{ar}	54.7	60.4	63.6	64.8	56.7	65.5	59.6	53.6	57.4
H_{α}	30.5	26.6	26.0	27.8	29.8	19.7	30.1	26.5	23.0
H_{o}	14.9	13.0	10.5	7.4	13.5	14.8	10.3	19.8	19.7
f_a	0.82	0.85	0.86	0.86	0.84	0.87	0.84	0.83	0.85
H_{aru}/C_{ar}	0.69	0.71	0.72	0.73	0.66	0.66	0.78	0.63	0.63
σ	0.26	0.22	0.21	0.21	0.25	0.17	0.27	0.26	0.21
R_s	3.92	3.43	3.60	3.68	3.87	2.48	4.63	3.16	2.45
n	1.49	1.49	1.40	1.27	1.45	1.75	1.34	1.75	1.86
C_A	21.86	21.38	23.65	23.63	23.18	22.23	21.97	19.73	18.71
R_A	4.36	4.05	4.30	4.16	4.89	4.80	3.37	4.67	4.51

[a]See Table I for definition.

Table XXIV. Molecular Formulas of Asphaltenes after Isothermal Reactions at 705°, 760° and 820° F

Sample	Molecular Formula
24-1	$C_{27.74}H_{21.62}N_{0.57}O_{0.62}S_{0.09}$
14-2	$C_{34.92}H_{26.31}N_{0.73}O_{0.86}S_{0.07}$
24-3	$C_{26.72}H_{20.09}N_{0.54}O_{0.54}S_{0.06}$
25-1	$C_{28.10}H_{21.32}N_{0.58}O_{0.54}S_{0.10}$
15-3	$C_{32.91}H_{24.29}N_{0.71}O_{0.88}S_{0.10}$
15-4	$C_{37.29}H_{30.02}N_{0.72}O_{1.31}S_{0.06}$
25-4	$C_{28.14}H_{21.58}N_{0.62}O_{0.81}S_{0.08}$
17-1	$C_{33.24}H_{25.03}N_{0.65}O_{1.17}S_{0.07}$
17-4	$C_{28.38}H_{21.32}N_{0.62}O_{1.05}S_{0.06}$
17-5	$C_{30.12}H_{22.27}N_{0.65}O_{1.16}S_{0.06}$
18-2	$C_{29.10}H_{21.12}N_{0.59}O_{0.54}S_{0.07}$
18-3	$C_{31.28}H_{23.46}N_{0.63}O_{0.90}S_{0.11}$
19-1	$C_{28.06}H_{20.52}N_{0.57}O_{0.52}S_{0.12}$
19-3	$C_{35.47}H_{25.99}N_{0.72}O_{0.69}S_{0.12}$
38-1	$C_{26.49}H_{20.52}N_{0.56}O_{0.79}S_{0.08}$
37-2	$C_{25.24}H_{19.60}N_{0.52}O_{0.82}S_{0.08}$
37-3	$C_{27.48}H_{21.14}N_{0.55}O_{0.85}S_{0.05}$
37-4	$C_{27.32}H_{21.03}N_{0.55}O_{0.75}S_{0.08}$
37-5	$C_{27.56}H_{20.32}N_{0.55}O_{0.84}S_{0.08}$
37-7	$C_{25.41}H_{18.52}N_{0.56}O_{0.65}S_{0.05}$
38-3	$C_{26.22}H_{21.12}N_{0.53}O_{0.44}S_{0.05}$
38-4	$C_{23.70}H_{17.21}N_{0.49}O_{0.87}S_{0.09}$
38-7	$C_{22.12}H_{16.09}N_{0.40}O_{0.60}S_{0.02}$

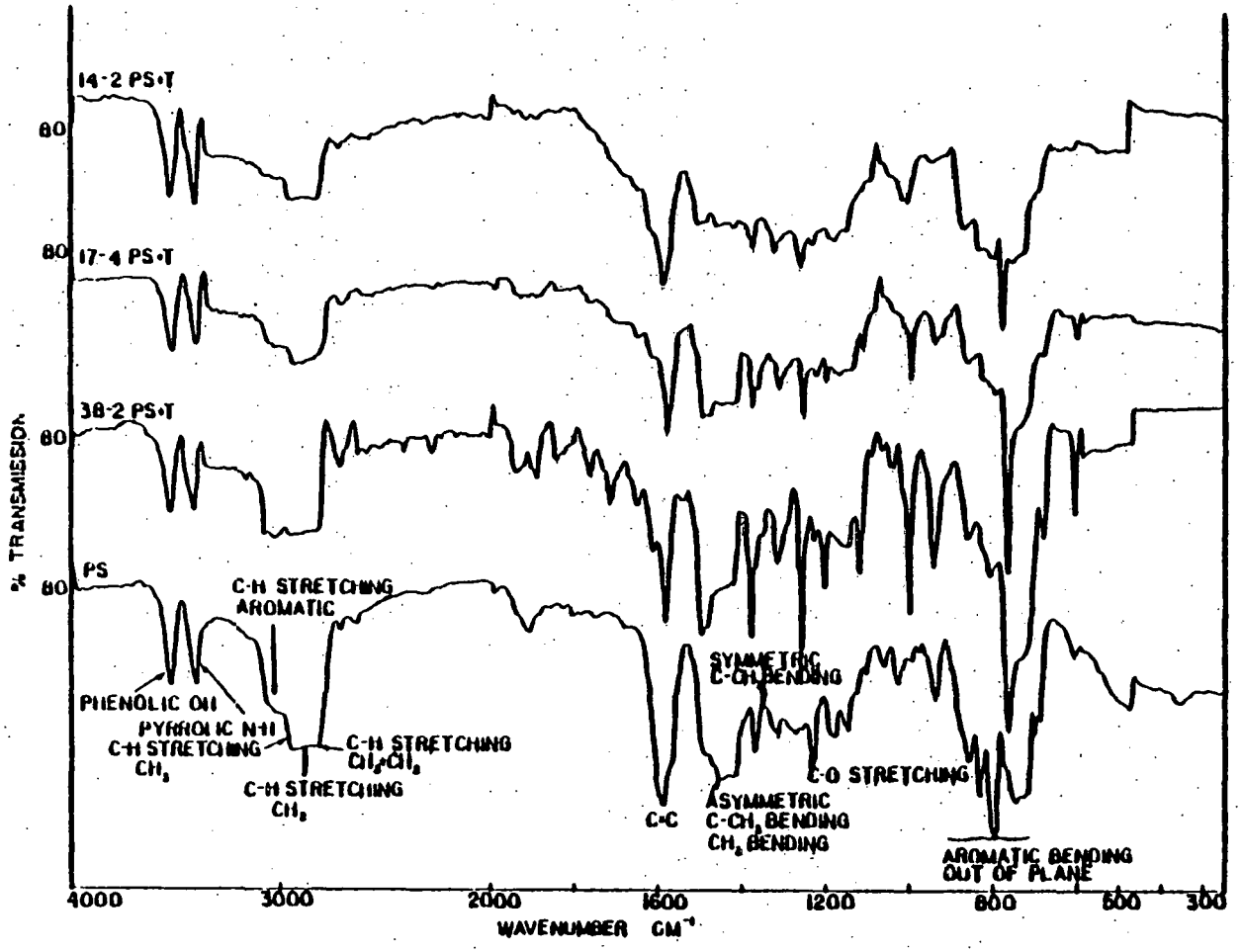

Figure 9. IR Spectra of PS and PS+T Fractions

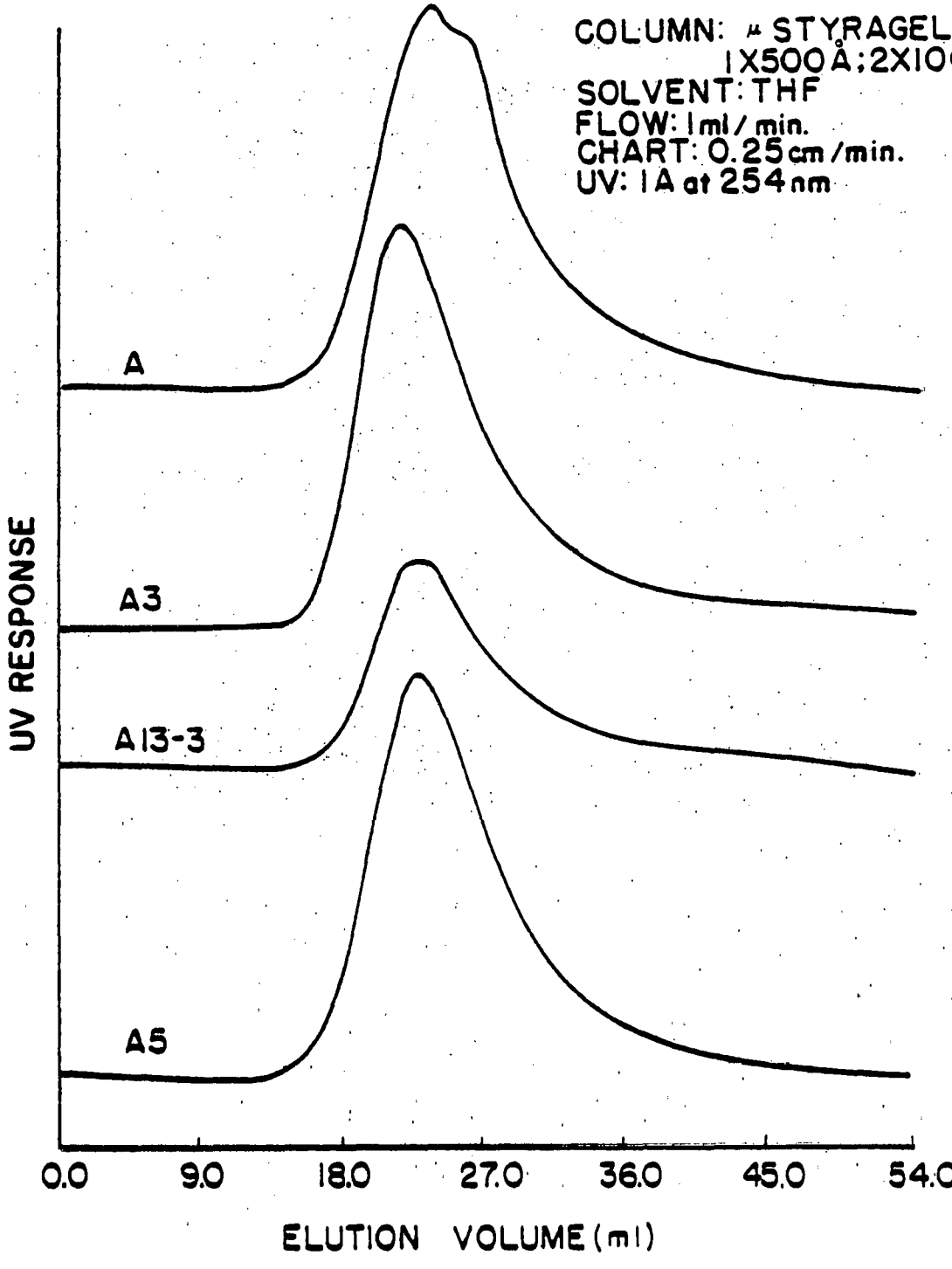

Figure 10. GPC Chromatograms of Asphaltenes

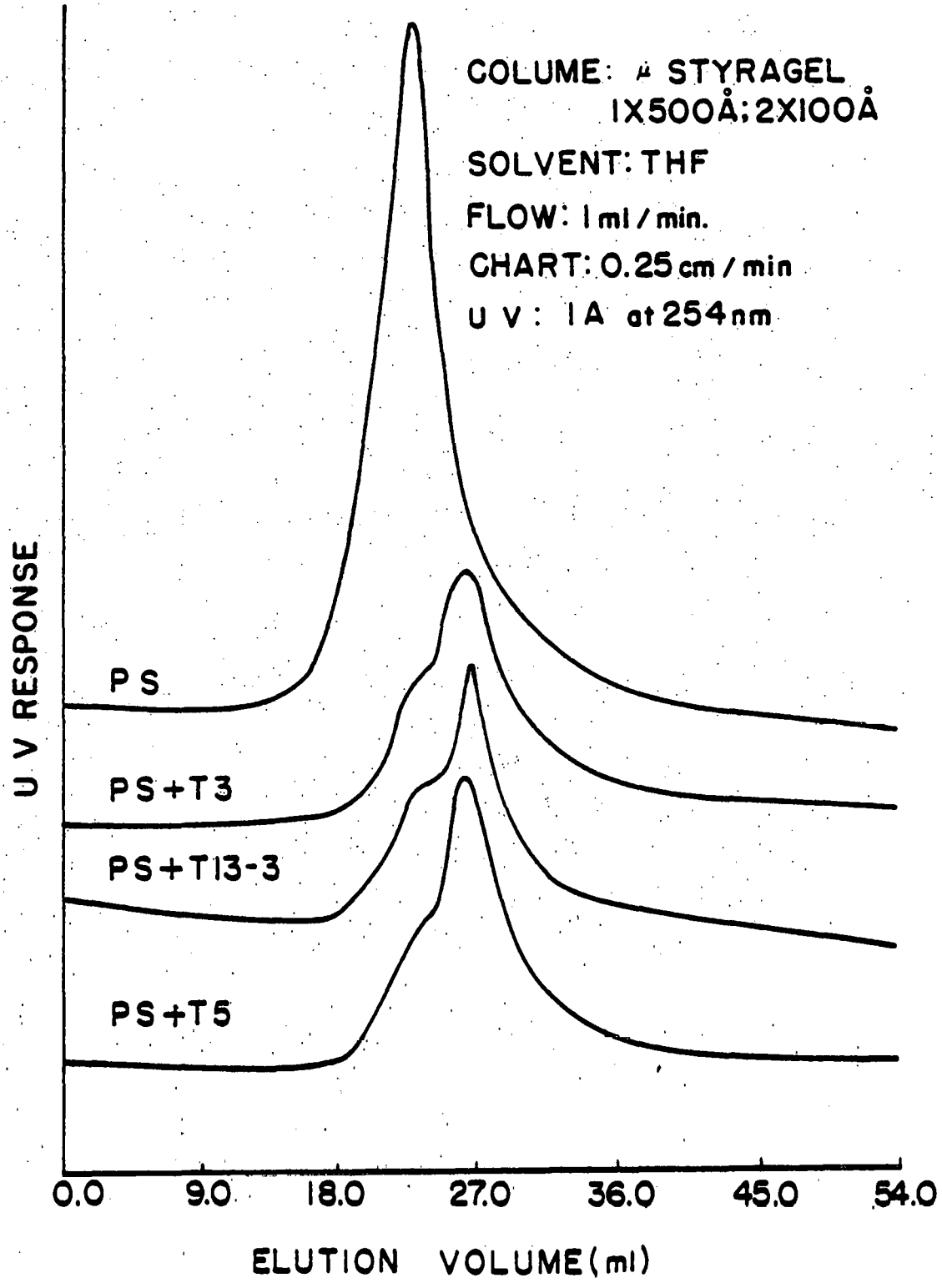

Figure 11. GPC Chromatograms of PS and PS+T Fractions

All PS + T fractions have been analyzed in the C_{18} column of HPLC. Representative chromatograms of PS + T fractions from isothermal reaction products at 760°F, are shown in Figure 12. The peak heights in cm of all PS + T fractions at elution volumes of 8.6, 10.8 and 14.8 ml are shown in Tables XXV to XXVII.

In order to study the role of tetralin in the reaction system, Run Nos. 22 and 40 have been carried out with tetralin as a reactant. The products were sampled and analyzed by HPLC with the C_{18} column. The reaction conditions and the peak heights in cm of all products at elution volumes of 8.6, 10.8 and 14.8 ml are shown in Tables XXVIII and XXIX. Figure 13 shows the chromatograms of all products from Run No. 22.

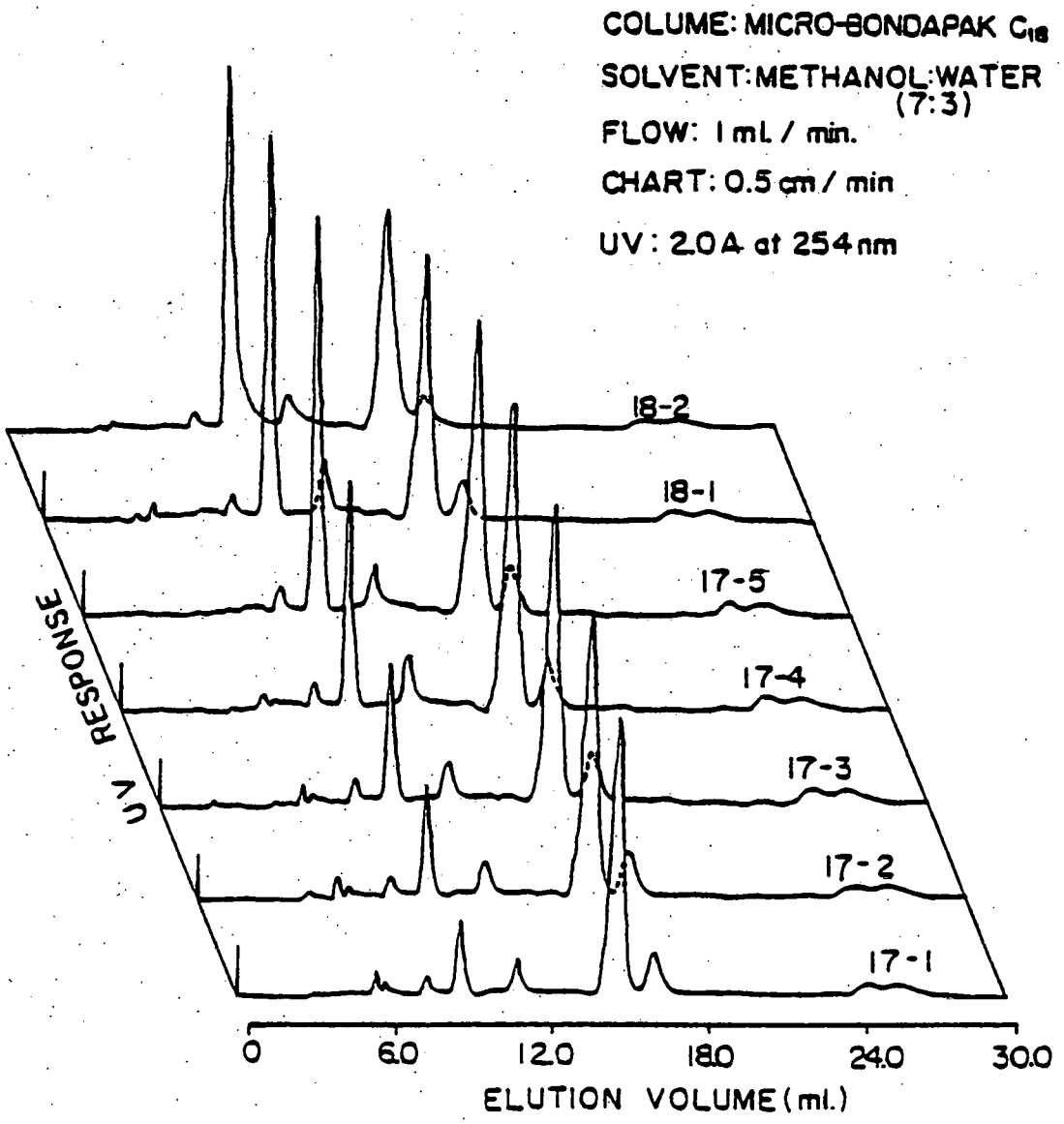

Figure 12. C_{18} Chromatograms of PS+T Fractions from Isothermal Reaction at 760^{0} F

Table XXV. C_{18} Chromatogram Peak Heights (cm) of PS+T Fractions from Isothermal Reaction Products at 705° F

PS+T from Run No.	Peak Height (cm) 8.6[a]	10.8[a]	14.8[a]	Peak Height Ratio 8.6/14.8	10.8/14.8
24-1	1.8	1.2	3.9	0.46	0.31
14-1[b]	1.2	0.8	4.8	0.25	0.17
	1.4	0.8	5.8	0.24	0.14
24-2	4.0	1.3	3.8	1.05	0.34
14-2	1.7	1.0	5.0	0.34	0.20
24-3	7.0	1.1	3.9	1.80	0.28
15-1	1.8	0.6	4.8	0.38	0.13
25-1	2.6	1.0	4.1	0.63	0.24
15-2	1.9	0.6	4.5	0.42	0.13
15-3	2.0	0.7	4.7	0.43	0.15
25-2	3.6	1.1	5.3	0.68	0.21
39-1[b]	1.75	0.6	2.5	0.70	0.24
	1.80	0.6	2.8	0.64	0.21
15-4	1.9	0.5	3.7	0.51	0.14
25-3	3.1	0.9	4.2	0.74	0.21
25-4	3.3	1.5	3.5	0.94	0.43
39-2[b]	3.7	1.2	2.9	1.28	0.41
	3.4	1.0	2.8	1.21	0.36
	3.9	1.2	3.4	1.17	0.36
	6.3	2.7	5.5	0.92	0.39
39-3	5.8	2.0	2.8	2.07	0.71

[a]Elution volume in ml.

[b]Independent runs.

Table XXVI. C_{18} Chromatogram Peak Heights (cm) of PS+T Fractions from Isothermal Reaction Products at 760° F

Ps+T from Run No.	Peak Height (cm) 8.6[a]	10.8[a]	14.8[a]	Peak Height Ratio 8.6/14.8	10.8/14.8
17-1[b]	1.48	0.7	5.5	0.27	0.13
	1.50	0.8	5.6	0.27	0.14
17-2	2.27	0.77	5.73	0.40	0.13
17-3[b]	2.76	0.85	5.90	0.47	0.14
	2.89	0.91	6.07	0.48	0.15
17-4	4.61	1.12	6.16	0.75	0.18
17-5	8.0	1.1	5.92	1.35	0.19
18-1	7.75	1.28	5.40	1.44	0.24
18-2	7.33	0.8	4.46	1.64	0.18
18-3	15.98	1.16	5.7	2.80	0.20
19-1[b]	17.80	1.36	9.41	1.89	0.15
	11.29	0.81	5.59	2.02	0.15
19-2	13.09	0.63	5.31	2.47	0.12
19-3	19.42	0.78	6.70	2.90	0.52
19-4	17.30	0.65	4.0	4.33	0.16

[a]Elution volume in ml.

[b]Independent runs.

Table XXVII. C_{18} Chromatogram Peak Heights (cm) of PS+T Fractions from Isothermal Reaction Products at 820° F

PS+T from Run No.	Peak Height (cm) 8.6[a]	10.8[a]	14.8[a]	Peak Height Ratio 8.6/14.8	10.8/14.8
37-1	2.2	0.9	3.8	0.58	0.24
38-1	1.2	0.9	1.8	0.68	0.50
37-2	3.3	1.0	3.5	0.94	0.29
37-3	2.9	1.3	1.9	1.53	0.68
37-4	7.5	1.9	4.3	1.74	0.44
37-5	4.3	2.9	1.8	2.39	1.61
37-6	5.2	2.7	1.5	3.47	1.80
37-7	13.4	5.4	4.0	3.35	1.35
38-3	5.5	3.0	2.2	2.50	1.36
38-4	5.3	2.5	1.6	3.31	1.56
38-5	6.0	2.8	1.9	3.16	1.47
38-6[b]	6.2	3.3	2.0	3.10	1.65
	6.5	4.8	2.96	2.96	1.96

[a]Elution volume in ml.

[b]Independent runs.

Table XXVIII. Reaction Conditions and C_{18} Chromatogram Peak Heights (cm) of Reaction Products of Run No. 22

(Reactant: Tetralin Only Pressure: 800 psig of N_2)

Sample	Temp. °F	Time (hr)	Peak Height (cm) 8.6[a]	Peak Height (cm) 14.8[a]	Peak Height Ratio 8.6/14.8
22-1	650	——	0.5	8.9	0.06
22-2[b]	700	——	0.3	6.1	0.05
			0.3	6.4	0.05
22-3[b]	760	0.0	0.4	6.5	0.06
			0.5	8.0	0.06
22-4	760	0.5	0.5	5.5	0.09
22-5	760	1.0	0.55	4.8	0.12
22-6	760	2.0	1.4	6.1	0.23
22-7	760	3.0	1.6	5.9	0.27
22-8	760	3.5	2.2	6.0	0.37
22-9	760	4.0	2.1	5.6	0.38
22-10[b]	760	20.42	5.85	5.55	1.05
			5.9	5.6	1.05

[a]Elution volume in ml.

[b]Independent runs.

Table XXIX. Reaction Conditions and C_{18} Chromatogram Peak Heights (cm) of Reaction Products of Run No. 40

(Reactant: Tetralin Only Pressure: 800 psig of N_2)

Sample	Temp. °F	Time (hr)	Peak Height (cm) 8.6[a]	10.8[a]	14.8[a]	Peak Height Ratio 8.6/14.8	10.8/14.8
40-1	700	—	0.9	0.2	0.9	1.00	0.22
40-2	820	0.00	3.4	0.3	3.5	0.97	0.09
40-3	820	0.25	3.3	0.2	3.1	1.07	0.07
40-4[b]	820	0.50	4.0	0.3	2.8	1.43	0.11
			3.0	0.3	2.4	1.25	0.13
40-5	820	0.75	3.1	0.4	3.2	0.97	0.13
40-6	820	1.00	2.1	0.4	2.5	0.84	0.16
40-7	820	2.00	3.6	0.9	3.4	1.06	0.27
40-8	820	3.00	2.1	1.1	3.0	0.70	0.37
			2.1	1.2	3.4	1.62	0.35
40-9	820	4.00	2.3	0.7	1.2	1.92	0.58
40-10	820	5.00	1.9	0.9	1.5	1.27	0.60
40-11	820	7.00	2.4	1.6	1.8	1.33	0.89
40-12	820	11.00	1.8	1.9	1.3	1.39	1.46
40-13	820	16.43	2.0	4.4	3.3	0.61	1.33
40-14	820	18.00	2.1	4.9	3.6	0.58	1.36
40-15[b]	820	21.00	1.5	4.8	2.1	0.71	2.29
			2.0	5.1	2.6	0.77	1.96
40-16	820	24.00	1.5	2.9	1.2	1.25	2.42

[a]Elution volume in ml.

[b]Independent runs.

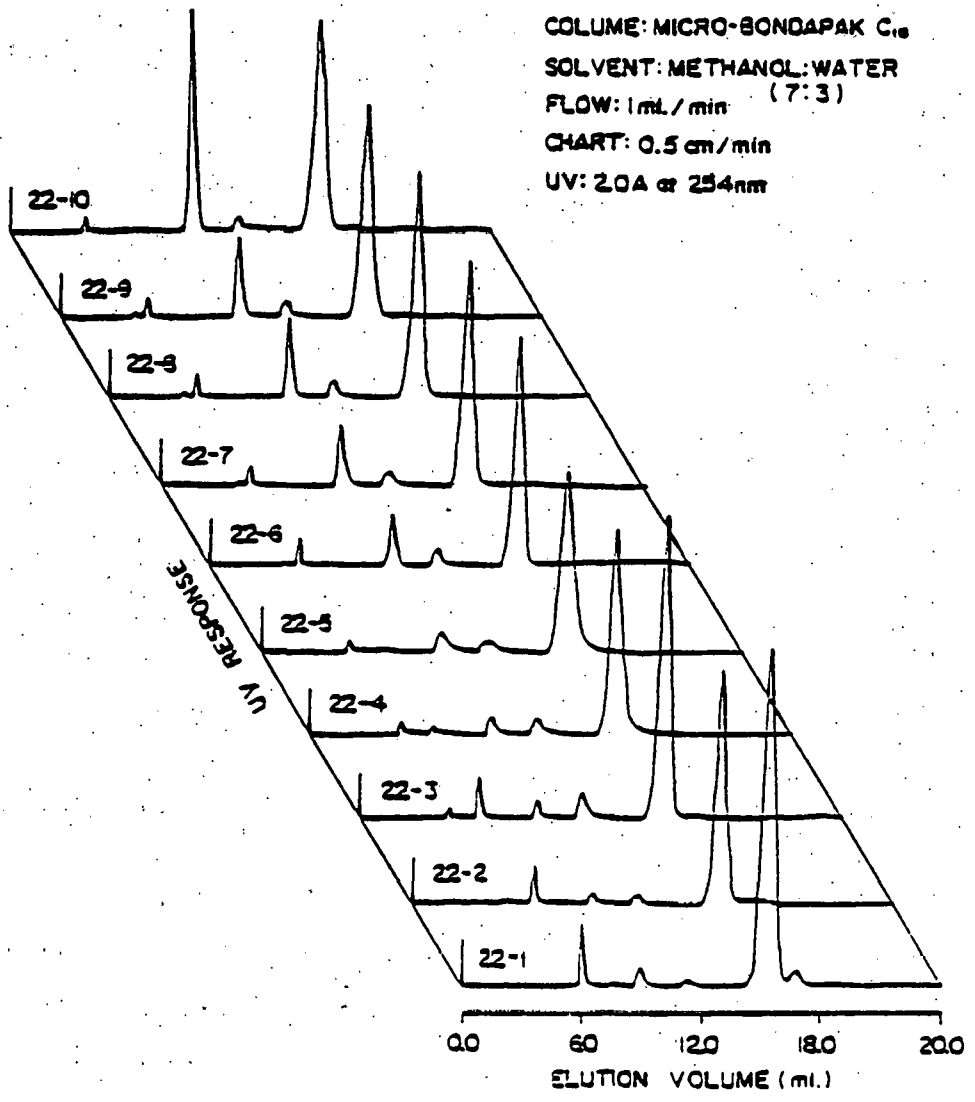

Figure 13. C_{18} Chromatograms of Reaction Products from Run No. 22

C. Discussion of Results

1. Precision of Experimental Results

All mass recoveries of 17 independent runs of solvent fractionation of SRC II stripper bottom, shown in Table III, are over 95% with an average yield of 98.1%. The standard deviation of each fraction obtained is within 8.6%.

The mass recoveries of 46 of the 54 separation runs of reaction products, shown in Table IV are over 90% with an average yield of 94.3%. The standard deviation is about 5.0%.

The results in Table V show the mass recoveries of all 18 reaction runs. In Run 16, the possible reason for the low recovery is gas formation from pyrolyzing A without tetralin. This is not within the scope of this study and therefore will not be discussed further. For other runs with low recovery, such as Run No. 5,24,37,38 and 39, tetralin vapor escaped when a series of products were sampled at different reaction times. This is the main reason why the recovery is low. In spite of these, the mass recoveries of 12 out of 18 runs are over 90%. The average recovery is 90.4%. This is fairly good, and indicates that it is reliable in terms of mass recovery. In addition, it is a system that can furnish a very close isothermal temperature profile, and provide meaningful definition of reaction time.

In order to check the precision of the reaction results, several products have been sampled from different runs under the same reaction conditions. The distributions of those products are shown in Table XXX. The results indicate that the average total standard deviation of the product distribution is 7.2%. This probably represents the total standard deviation of the whole experiment, including the temperature, reaction and separation variations.

The error of elemental analyses of carbon, hydrogen, nitrogen, sulfur and ash are reported to be $\pm$ 0.3%, while that of molecular weights obtained by extrapolating to infinite dilution to be $\pm$ 7.8%.[4]

Since NMR, IR and HPLC are quite sophisticated modern instruments, the results obtained should be reasonably reliable.

2. Comparison Between Autoclave Reaction and Kinetic Model

According to the model presented in Chapter 5.3, the following relationships are anticipated to yield straight lines:

$0 < t \leq t_1$

Log A vs. t
PS vs. PS + BI

$t_2 < t$

Log A vs. t
Log BI vs. t

The slopes of above straight lines are related to the four rate constants in the following ways: when $0<t\leq t_1$, the slope of Log A vs. t is equal to $-(k_1 + k_3)/2.3$, and that of PS vs. PS + BI is $k_1/(k_1+k_3)$; when $t_2<t$, the slope of Log A vs. t is equal to $-k_2/2.3$, and that of Log BI vs. t is $-k_4/2.3$.

The experimental data from isothermal reactions at 705°, 760°, and 820° F have been tested according to the above relationships, and are shown in Figures 14 to 15. Computer-assisted least squares fit has been used to treat those experimental data. The resulting straight lines are plotted in the corresponding figures and shown in Table XXXI. The standard deviations of the ordinates, slopes, and intercepts of the lines, along with correlation coefficients are also included. Confidence limits of these slopes have been analyzed by the method in Chapter 8 of Reference 41. For a 70% confidence level, equal to or less than a ±40% interval of these slopes have been obtained for nine out of twelve equations in Table XXXI. The other three equations, i.e., first, third, and seventh, have much higher intervals for the same percentage confidence level.

Since the first and third equations are involved in the first stage of the reaction, the experimental data are considered scattered higher in the first stage than the other two stages. A plausible reason is that the temperature in the first stage was not so stable as in the later stages. Another fact is that the reactions in the first stage are so fast that they are much harder to track.

Several other models have been tested to fit the experimental data, for example, the model with three rate constants in one stage, the model with four rate constants in two stages, or the model with four rate constants in three stages, but with only one rate constant in the second stage. However, the result obtained is much better from the current model than from the other three models. Under this circumstance, the interconversion of coal-derived products studied in this research can therefore be reasonably represented by the model proposed in Chapter 5.3, with four first-order rate constants with three stages.

With a sophisticated reactor system developed in the future, more reliable data could be obtained to quantify this model more precisely, and hopefully a better modified model could also be developed to fit the experimental data.

According to the model proposed, the rate constants can be calculated from the slopes of the lines in Table XXXI. The values of these four rates constants obtained are shown in Table XXXII.

The rate constant, k_3, can also be obtained from the slope of the line: when $t_1< t \leq t_2$, the slope of Log A vs. t is equal to $-k_3/2.3$. The experimental data in the second stage at 705°F have been plotted according to the above relationship and shown in Figure 16. The least squares fit line, with accompanying standard deviations of the ordinate, slope, and intercept of the line, along with correlation coefficient, is also presented in Figure 17. For a 70%

confidence level, ± 35% interval of this slope is obtained from statistical analysis. [41] The rate constant, k_3, obtained by this method is about 101.0% higher than the value obtained from the first stage. This percentage is assumed for the percentage variation of k_3 for all three temperatures. The variations of other rate constants are obtained from the standard deviations of the slopes of the least-squares fit lines. Those variations are also presented in Table XXXII. Since the rate constants k_1 and k_3, show larger variations than k_2 and k_4, and k_1 and k_3 are the main rate constants for the first stage of the reaction, the result concluded for the first stage is less precise than for the other two stages. The numbers presented in Table XXXII for the rate constants are only considered as semi-quantitative, because of their large variations.

Since analytical solutions of rate equations were known for each section of the model, the rate constants were substituted into the analytical solutions, i.e. Equations 17 to 25 to calculate the product distributions. A computer program shown in Appendix as Program 4 was used for this calculation. Curves were generated to represent the theoretical trends for PS, A, and BI. These curves were plotted on the same coordinates with experimental data, as shown in Figures 5 to 7 . The calculated curves for the conversion of A, and the productions of PS and BI vs. time agree reasonably well with the experimental data for all three isothermal reactions. Standard deviations of the calculated values with respect to the experimental data have also been obtained in the Program 4. They are 16.1%m 14.5% and 10.7% for isothermal reactions at 705°, 760°, and 820°F, respectively. The main variations for reactions at 705°, 760°F concentrate on the first one or two points in the first stage when the reaction time is short ($t < 0.5$ hr). Without these points, the standard deviations are much improved, and are 7.8% for 705°F and 8.0% for 760° F.

All rate constants in Table XXXII show temperature variations. Assuming on Arrhenius dependency, the relations of Ln(ki) vs. (1/temp) are shown in Figure 18, together with the least-squares fit lines. The equations of those lines, and standard deviations of the ordinates, slopes, and intercepts, along with correlation coefficients, are presented in Table XXXIII. The statistical analysis method in Chapter eight of Reference 41 has also been used to test the confidence intervals of those equations. It has been found out that about ±45% of the activation energies can be obtained for a 60% confidence level for those four equations. The values of activations energy and frequency factor are calculated from the slopes and intercepts. Those values as well as their uncertainties obtained from standard deviations of the corresponding slopes and intercepts are also listed in Table XXXIII. The result incicates that the simple Arrhenius relation seems to hold for all four kinetic rate constants over the temperature range studied.

Table XXX. Standard Deviation of Product Distribution

Run No.	PS	PS(Ave.)	Sd_1[a]	A	A(Ave.)	Sd_2[a]	BI	BI(Ave.)	Sd_3[a]	Sd_s[b]
14-2	34.2	40.6	6.4	59.9	50.7	9.1	5.9	8.8	2.9	11.5
24-3	46.9			41-4			11.7			
15-1	30.8	40.0	9.2	54.8	48.9	5.9	14.3	11.1	3.3	11.4
25-1	49.2			43.0			7.8			
25-2	32.3	33.2	0.9	56.1	55.2	0.9	11.6	11.6	0.0	1.3
39-1	34.1			54.3			11.6			
15-4	36.6	42.8	6.2	61.3	50.9	10.5	2.1	6.4	4.3	12.9
25-3	49.0			40.4			10.6			
17-5	48.1	49.0	0.9	44.7	43.8	1.0	7.1	7.2	0.1	1.3
18-1	49.9			42.8			7.3			
37-1	25.8	27.0	1.2	71.7	68.3	3.4	2.5	4.8	2.3	4.3
38-1	28.1			64.9			7.0			
37-4	26.7	32.8	6.1	63.8	60.5	3.4	9.5	6.8	2.7	7.5
38-2	38.8			57.1			4.1			
									Ave:	7.2

[a] Sd_1, Sd_2 and Sd_3: Standard Deviations of PS, A, and BI respectively.

[b] $Sd_s^2 = Sd_1^2 + Sd_2^2 + Sd_3^2$

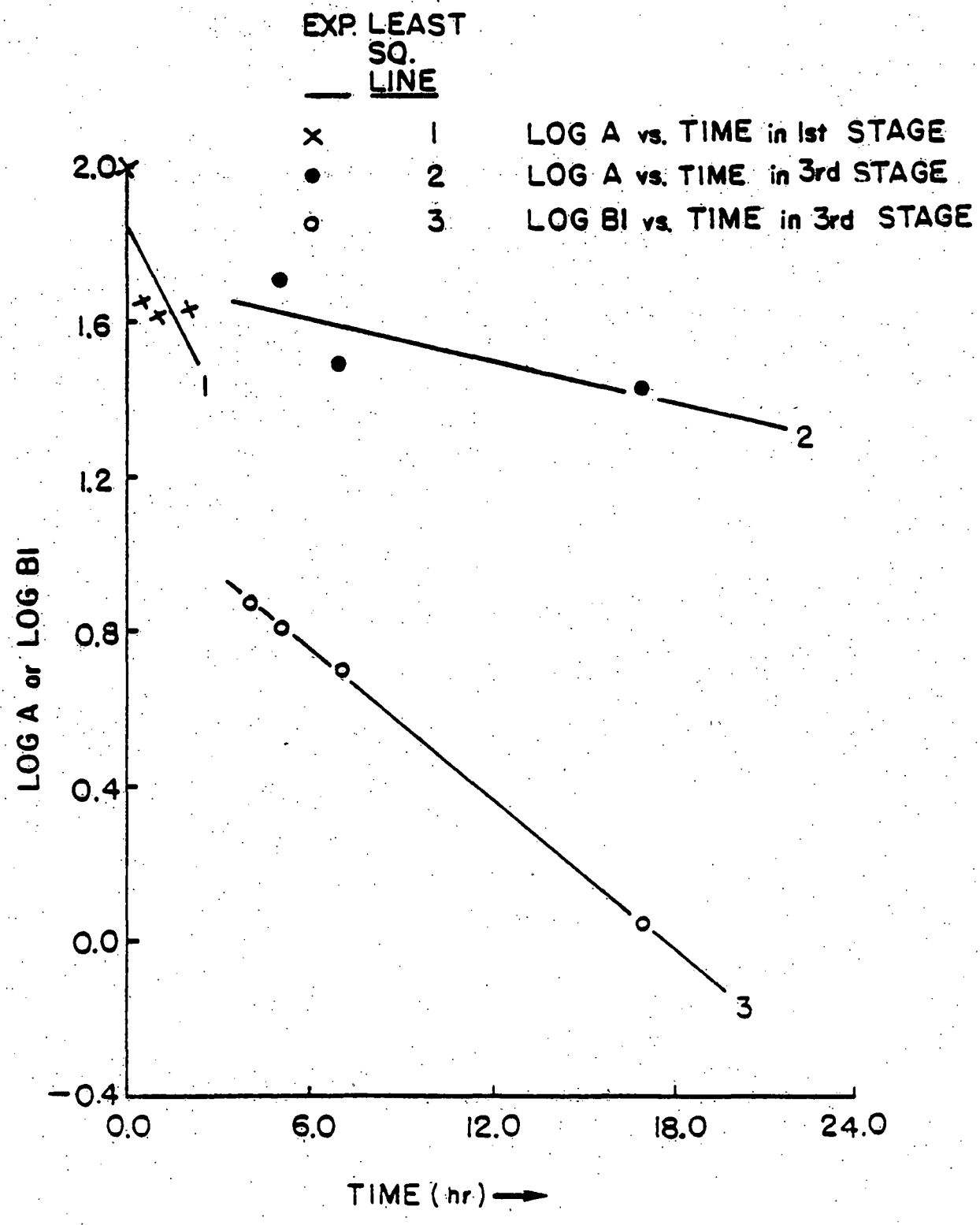

Figure 14. First Order Plot for Log A or Log BI va . Tiem at Different Stage at 705° F.

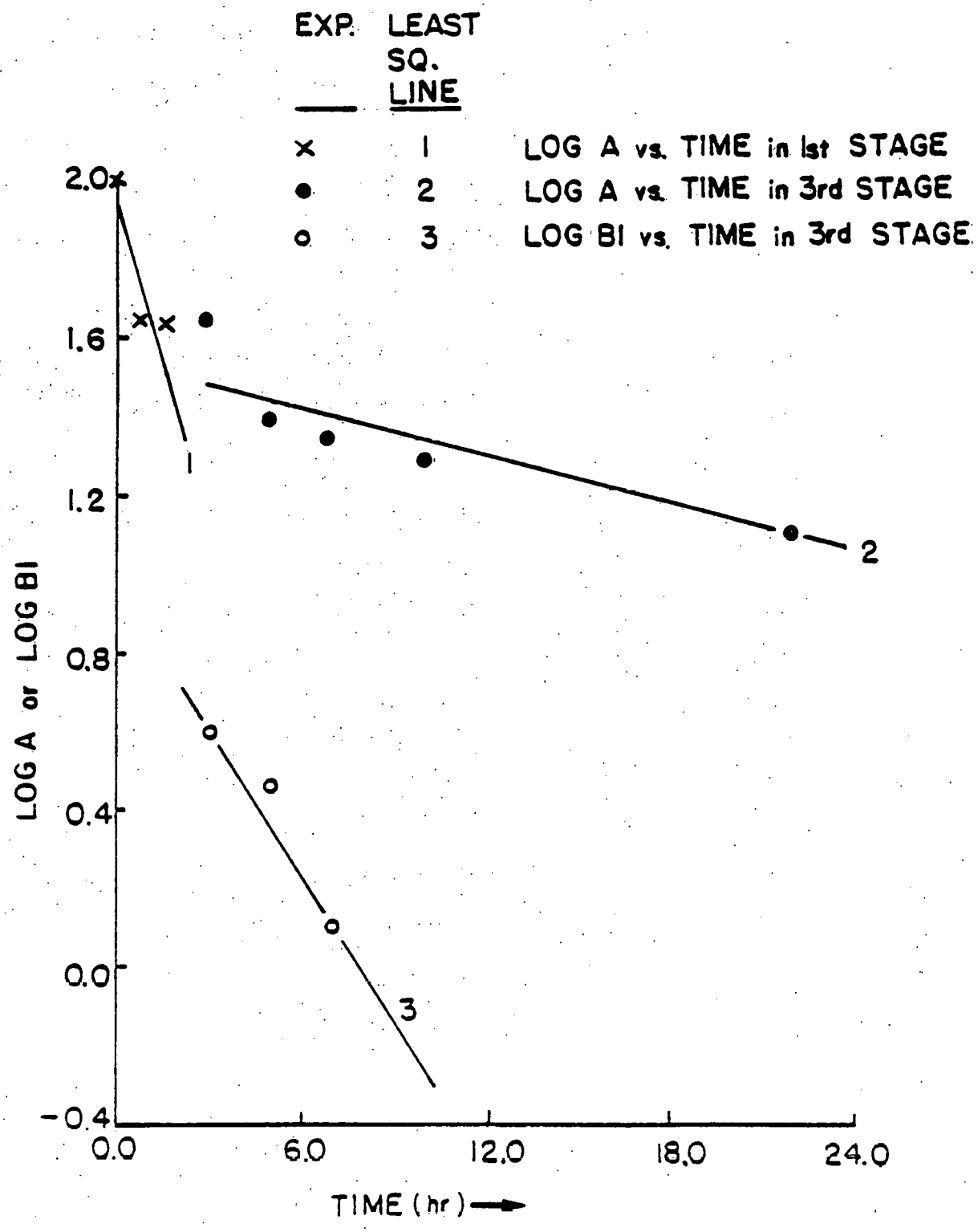

Figure 15. First Order Plot for Log A or Log BI vs. Time at Different Stage at 760° F

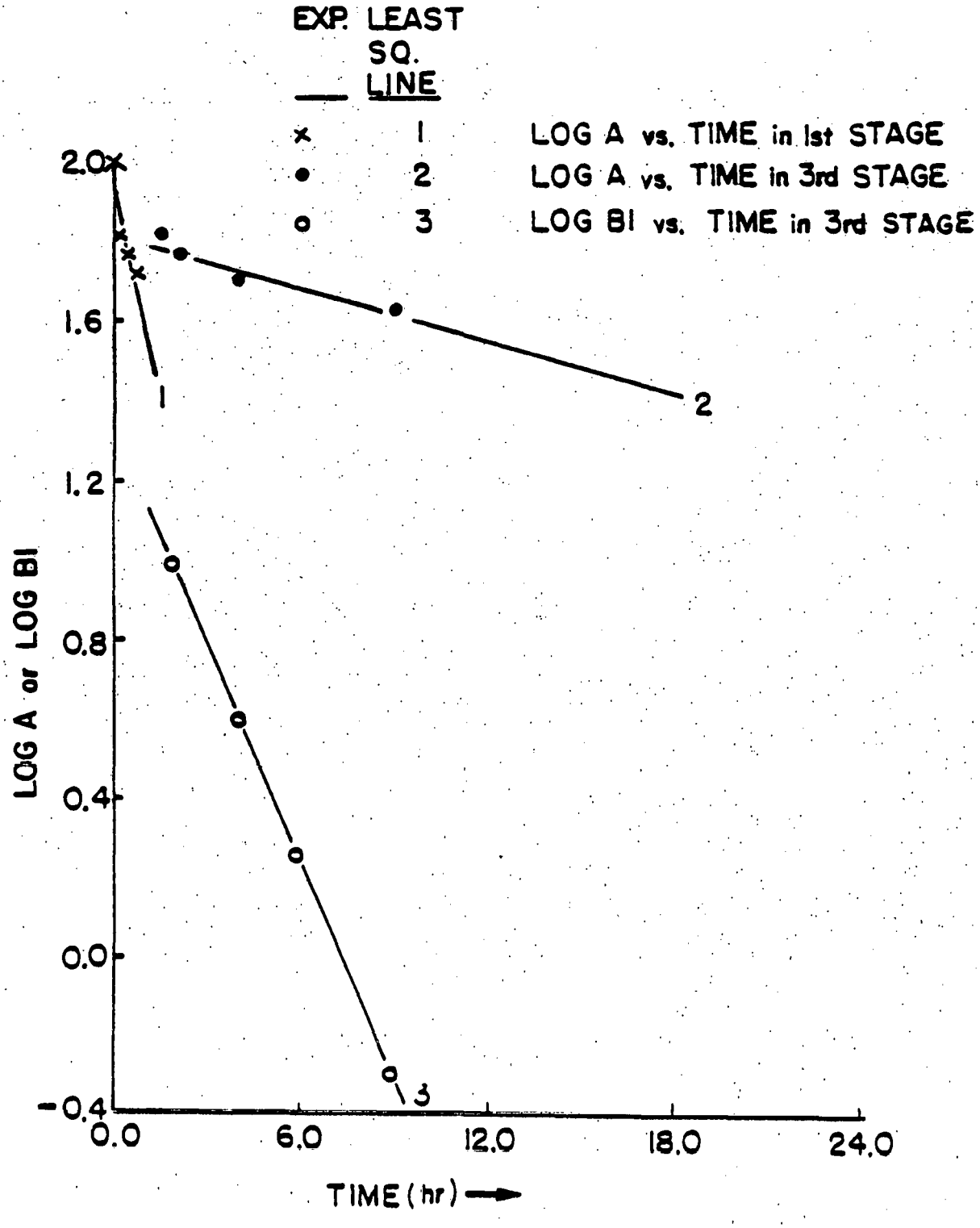

Figure 16. First Order Plot for Log A or Log BI vs. Tiem at Different Stage at 820° F

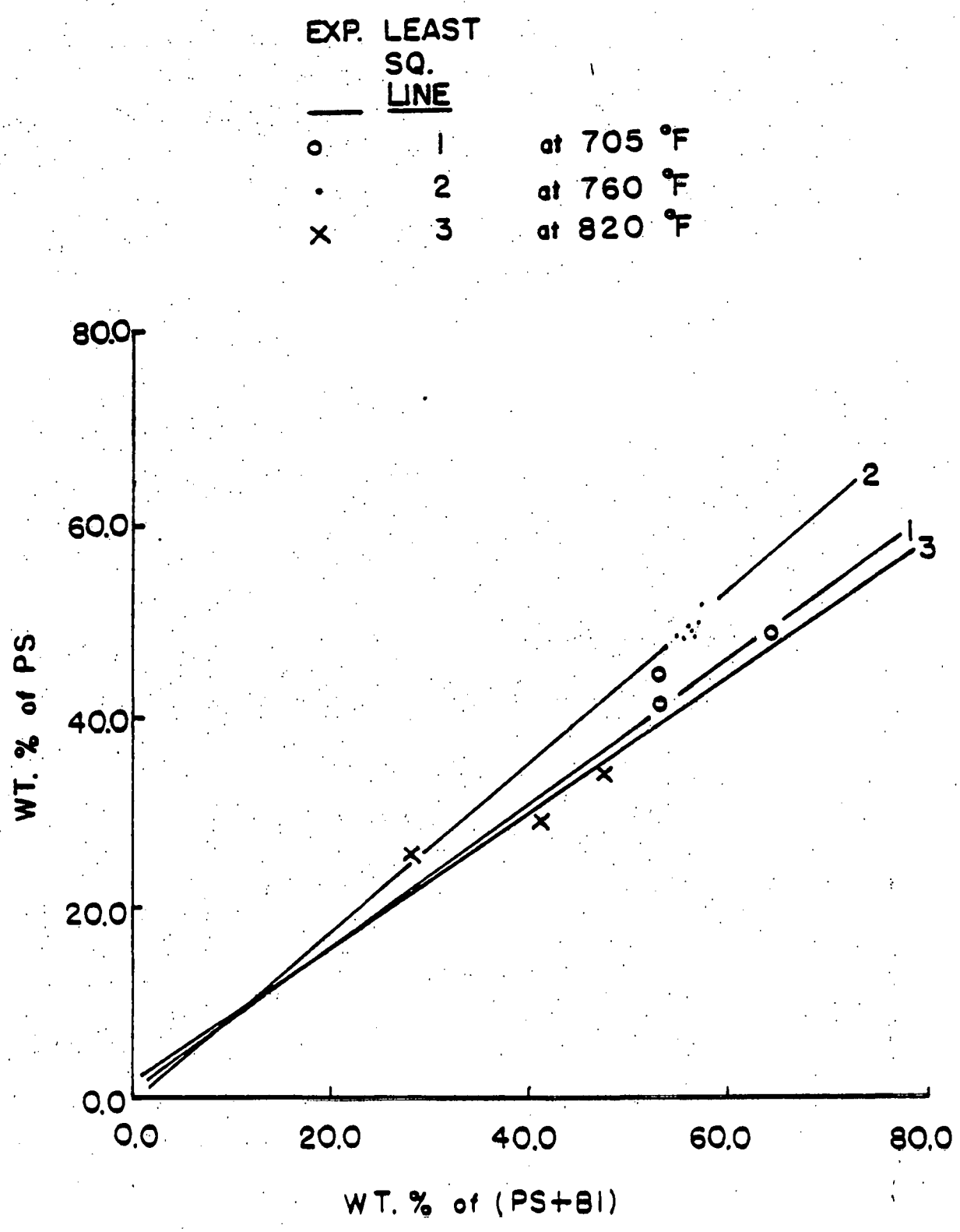

Figure 17. First Order Plot for PS vs. PS+BI at First Stage

Table XXXI. Least Squares Fit of Conversion Data vs. Time (hr)

Temp. (°F)	Least Squares Fit	Standard Deviation: Ordinate	Slope	Intercept	Corr. Coeff.	t_1[a] (hr)	t_2[b] (hr)
$0 < t \leq t_1$							
705	Log A = -0.149 t + 1.855	0.163	0.110	0.126	0.692	2.0	4.0
	PS = 0.771 (PS + BI) + 0.433	2.289	0.046	2.259	0.997		
760	Log A = -0.246 t + 1.942	0.142	0.133	0.129	0.879	1.5	3.0
	PS = 0.876(PS + BI) - 0.019	0.738	0.014	0.778	0.999		
820	Log A = -0.351 t + 1.954	0.045	0.079	0.034	0.932	0.75	1.5
	PS = 0.709(PS + BI) + 1.520	3.455	0.094	3.261	0.983		
$t_2 < t$							
705	Log A = -0.018 t + 1.709	-0.136	0.015	0.165	0.77	2.0	4.0
	Log BI= -0.064 t + 1.133	0.013	0.001	0.012	0.999		
760	Log A = -0.023 t + 1.565	0.108	0.007	0.083	0.88	1.5	3.0
	Log BI= -0.123 t + 0.981	0.047	0.017	0.087	0.991		
820	Log A = -0.023 t + 1.803	0.035	0.006	0.030	0.938	0.75	1.5
	Log BI= -0.182 t + 1.335	0.019	0.004	0.021	0.99		

[a]Reaction time that separates stage one and two.

[b]Reaction time that separates stage two and three.

Table XXXII. Rate Constants (hr^{-1}) for Interconversion of Coal Derived Products

Temp.(^{o}F)	$k_1 \cdot 10^{a}$	$k_2 \cdot 10^{2}$	$k_3 \cdot 10^{2}$ [a]	$k_4 \cdot 10$
705	2.65±3.33	4.09±3.41	7.86±7.94	1.47±0.02
760	4.95±3.78	5.29±1.61	7.02±7.09	2.82±0.38
820	5.72±4.18	5.29±1.39	23.52±23.76	4.18±0.08

[a]The uncertainty in both k_1 and k_3 are large. This is not unusual for coal-derived liquid kinetic studies, for example the uncertainty of some rate constants in Reference 39 are over 100%.

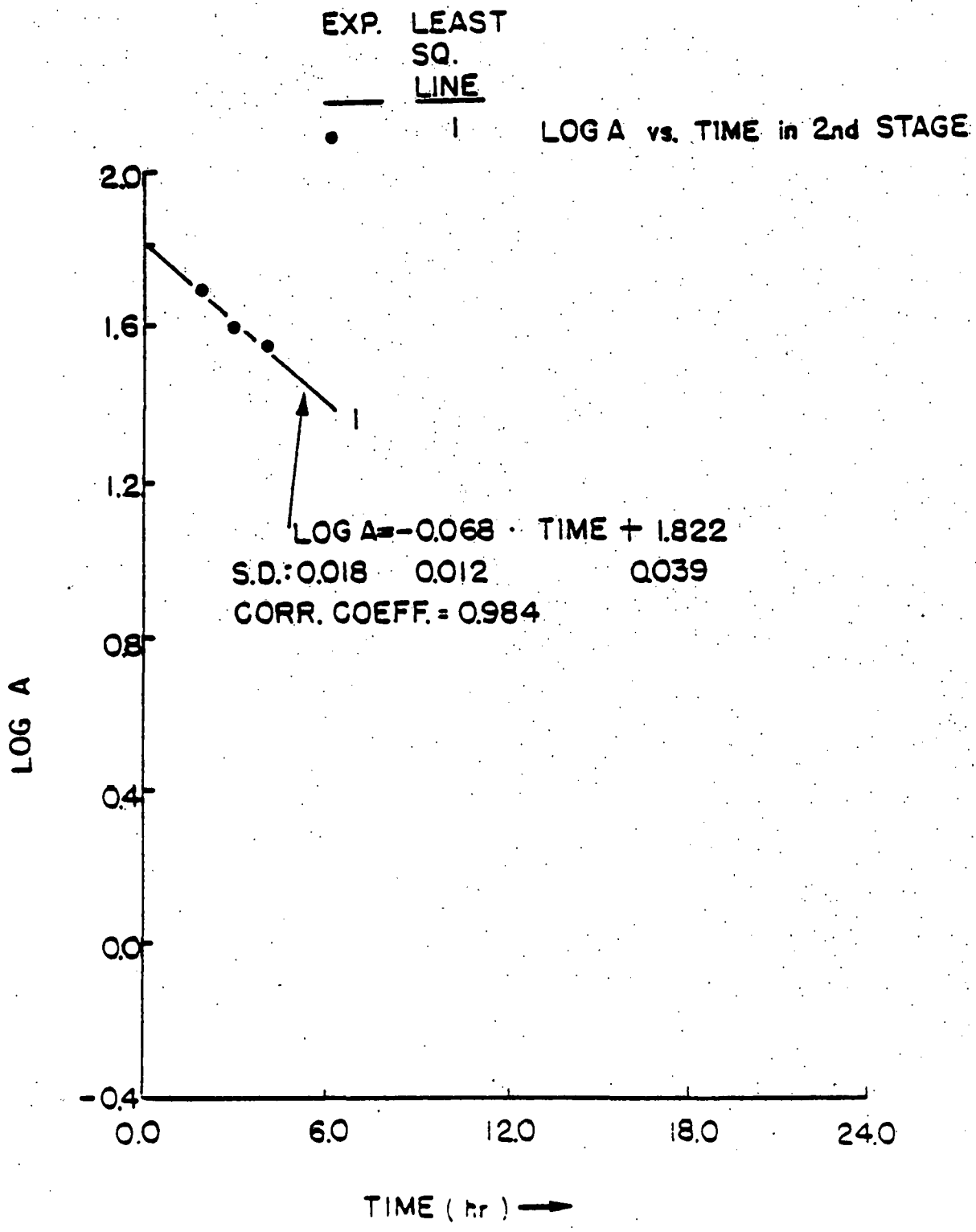

Figure 18. Semi-Log Plot for A vs. Time at Second Stage at 705° F

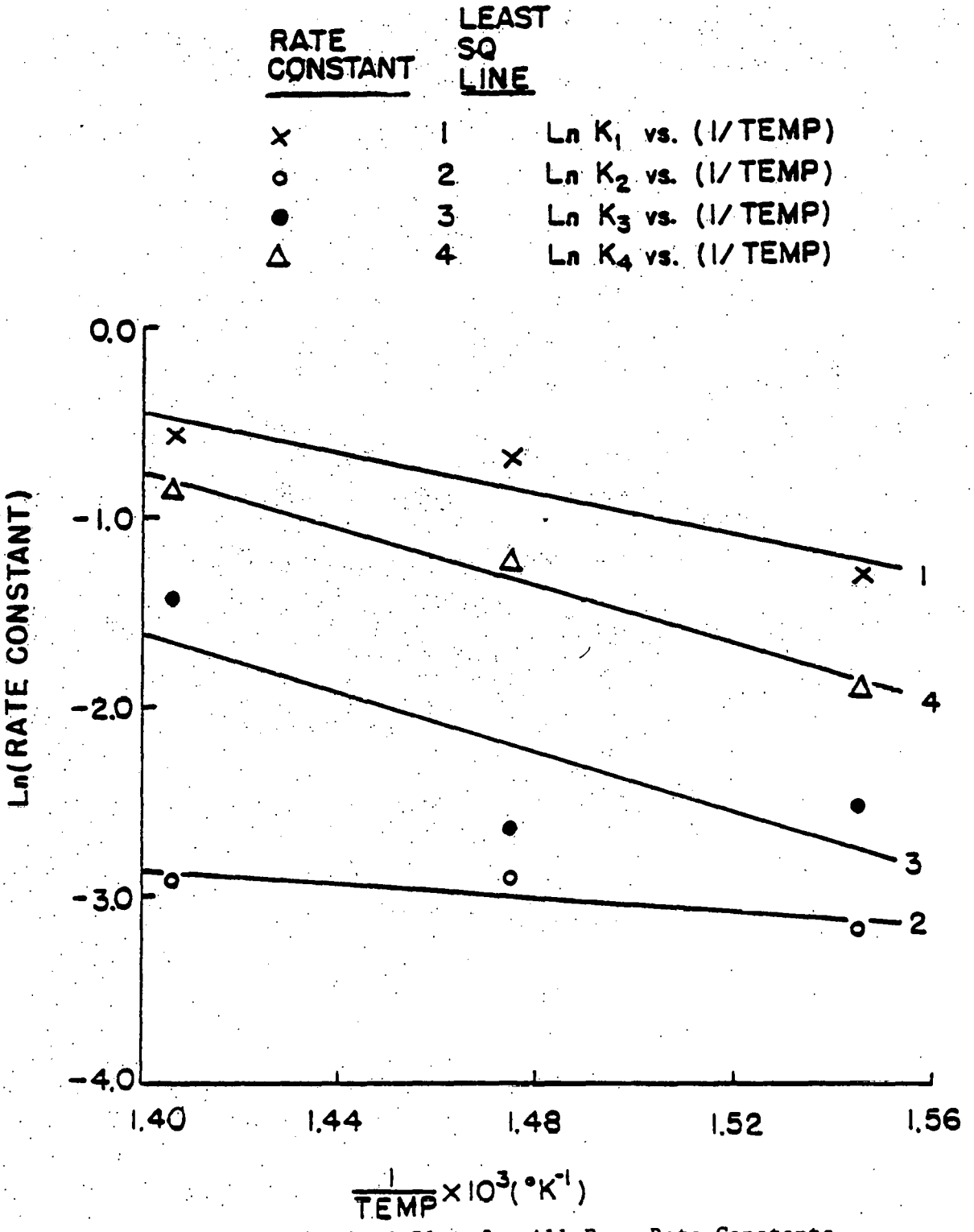

Figure 19. Arrhenius' Plot for All Four Rate Constants

The calculated activation energies together with the nearly developed kinetic model are shown in comparison with othe existing models in Table XXXIV. These existing models have already been discussed in detail in Chapter 2.3--c. The models of Weller et al.,[8-9] Curran et al.,[10] Yoshida et al.,[11] and Wen et al.[12] have been known to be inadequate because of the neglecting of the benzene-insoluble fraction. In Brunson's study,[13] the proposed model is based on the distillation results of coal liquids produced from the pilot plant of the Exxon Donor Solvent process. This definition of conversion is different from the rest of the studies. This leads to the large difference in the absolute value of conversion and in turn to the difference in the models proposed by other authors.

The model developed therein can probably be closely compared qualitatively with the work by Cronauer et al.[14] and Shalabi et al.[15] Data used in this study were obtained directly from conversions among pentane-soluble, asphaltene, and benzene-insoluble fractions, while in those two studies, coal was used as a starting reactant for the kinetic study, and the model for pentane-soluble, asphaltene, and benzene-insoluble fractions was based on presumed chemistry of the liquefaction process. The difference in the kinetic relationship between asphaltene and benzene-insoluble fractions could stem from this point. It is also one of the reasons why the activation energy of asphaltene to pentane-soluble fraction measured by Cronauer et al.[14] (E_5= 16.0 K-cal/g-mole) is different from that obtained in this work (E_1= 11.0 K-cal/g-mole). Among other possible reasons are the wide variety of the reactor type, vehicle solvent, catalyst, and measurement of conversion used among these two studies.

It is clear that the reactor type, vehicle solvent, catalyst, and measurement of conversion are varied among all the studies shown in Table XXXIV. No two studies have the exact same conditions for the kinetic study. Under this circumstance, even if there were two identical kinetic models proposed, it would not mean that the two can be compared unless the products were characterized by the same chemical methods. The chemical characterization of coal-derived products, although important, is lacking in most of the kinetic studies shown in Table XXXIV. It is the major concern in the later section of this study.

Since the large variations in determination and low confidence level in the statistical analysis, the data obtained for rate constants, activation energies, and frequency factors in this study are semi-quantitative. This is considered plausible because the coal-derived product is a very complicated system, probably involving hundreds of different compounds that react at the same time. Furthermore, the variations in this study are much more lower than other studies. For example, the variation of some rate constants in REference 39 is over 100% or 200%, and the variation of some activation energies in Reference 37 exceeds 100% to 200%. Therefore, the data obatined are more reliable from this study than from others for the interconversion

Table XXXIII. Least Squares Fit of Arrhenius Relation

Least Squares Fit	Standard Deviation			Corr. Coeff.	Activation Energy[a]		Frequency Factor
	Ordinate	Slope	Intercept		K-joule g-mole	K-cal g-mole	(hr^{-1})
$Lnk_1 = \frac{-5.54 \cdot 10^3}{temp} + 7.31$	0.19	$1.97 \cdot 10^3$	2.91	0.942	46.1 ±16.8	11.0 ±4.0	$1.50 \cdot 10^3$ ±1.84·10
$Lnk_2 = \frac{-1.85 \cdot 10^3}{temp} - 0.29$	0.10	$1.06 \cdot 10^3$	1.57	0.868	15.4 ±8.8	3.7 ±2.1	$7.51 \cdot 10_0^{-1}$ ±4.81·10
$Lnk_3 = \frac{-7.78 \cdot 10^3}{temp} + 9.39$	0.54	$5.52 \cdot 10^3$	8.16	0.818	65.4 ±46.5	15.6 ±11.1	$1.20 \cdot 10_3^4$ ±3.50·10
$Lnk_4 = \frac{-7.52 \cdot 10^3}{temp} + 9.75$	0.10	$1.04 \cdot 10^3$	9.75	0.991	62.5 ±8.6	14.9 ±2.1	$1.70 \cdot 10_0^4$ ±4.66·10

[a]The uncertainty of some activation energies in the coal liquefaction studies can exceed 100-200%, for example in Ref. 37.

Table XXXIV. Comparison of Kinetic Model and Activation Energy

REFERENCE	REACTOR	VEHICLE	CAT.	MEASURE OF CONVERSION	MODEL	ACTIVATION ENERGY (K-cal/g mole)
Weller et al. (Ref. 33,34)	Batch	No	Yes	n-Hexane Benzene	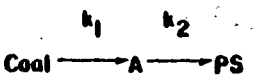	E_1 -- E_2 -35.8
Curran et al. (Ref. 10)	Batch	Tetralin	No	Xylenol	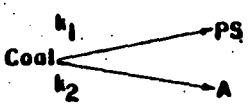	E_1 -30.0 E_2 -38.3
Yoshida et al. (Ref. 8)	Batch	Anthracene Oil	Yes	n-Hexane Benzene	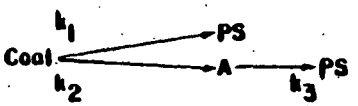	Not available
Wen et al. (Ref. 37)	Batch (U. Utah)	Coal-Derived Oil	No	Benzene		18.7
	Continuous Ebullated Bed (H-Coal)	Coal-Derived Oil	Yes	Benzene		3.3
	Continuous Dissolver (SRC-I)	Coal-Derived Oil	No	Benzene		1.4

Table XXXIV (Continued)

REFERENCE	REACTOR	VEHICLE	CAT.	MEASURE OF CONVERSION	MODEL	ACTIVATION ENERGY (K-cal/g mole)
Brunson (Ref. 40)	Flow Tubular (EDS)	Recycle Vehicle	No	Distillation	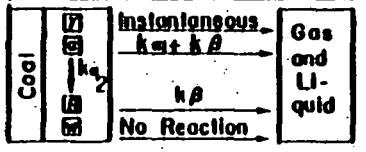	E_{α_1} - 38.5 E_{α_2} - 18.9 E_β - 15.9
Cronauer et al. (Ref. 38)	Continued Stirred Tank	Hydrogenated Anthracene Oil (AO) & Phenanthrene (PO)	No	Pentane Benzene Pyridine	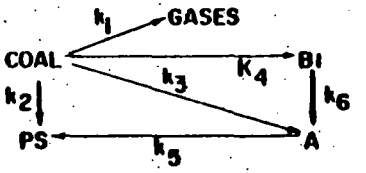	AO / PO E_1 - 21.5 / 10.5 E_2 - 14.1 / 28.9 E_3 - 15.6 / 8.6 E_4 - 13.8 / 4.3 E_5 - 16.0 / 25.6 E_6 - 12.8 / 32.9
Shalabi et al. (Ref. 39)	Batch	Tetralin	No	Pentane Benzene THF		E_1 - 40.0 E_2 - 29.0 E_3 - 30.0
Present Work	Batch	Tetralin	No	Pentane Benzene THF	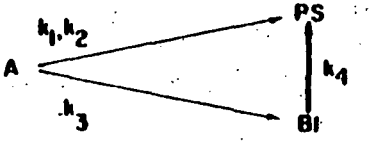	E_1 - 11.0 E_2 - 3.7 E_3 - 15.6 E_4 - 14.9

of coal-serived products. However, special caution must be taken in using these data.

Long reaction time of 24 hours has been used in this study, and the secondary reaction of asphaltene to pentane-soluble fractions at a later stage has been observed. This is the first time that a secondary reaction has been reported. This is the first time also that the interconversion of coal-derived products (PS,A, and BI) has been studied more thoroughly in experiments.

3. Justification of the Kinetic Model by the Independent Investigation in HPLC with a C_{18} Column

All the pentane-soluble and tetralin fractions (PS +T) obtained in this work for the kinetic study have been analyzed by the high pressure liquid chromatography (HPLC) using a reverse phase Micro-bondapak C_{18} column. The result shown in Tables XXV to XXIX and Figures 12 and 13 tends to support the kinetic model proposed above and is discussed in the following paragraphs of this section.

The C_{18} column is packed with materials having polarities increased from non-polar to high polarity. Molecules are separated through the column according to polarity. Non-polar molecules elute slower than high polar molecules since non-polar molecules are absorbed by the non-polar materials packed at the entrance of the column. The chromatograms shown in Figure 12 indicate a very good separation. There are very large and sharp peaks at elution volumes of 8.6,10.8, and 14.8 ml. The peak height at 8.6 ml seems to increase with reaction time for a isothermal run. Spiking experiments have been used to identify the peaks at 8.6 and 14.8 ml elution volumes as naphthalene and tetralin, respectively. Since naphthalene is more polar than tetralin, naphthalene elutes first. It is reported from literature[16] that naphthalene and 1-methyl-indan are major products when tetralin is heated without hydrogen or coal at temperatures between 630° and 842° F. It is seemed that the peak at 10.8 ml elution volume is 1-methyl-indan. The evidence is that this peak height increases as reaction goes in Run No. 40, where the tetralin alone was heated at 820° F for about 24 hours.

The peak height or peak area does not correspond to the mass contained, since the UV response is different for different compounds. Naphthalene is much more sensitive to UV response than tetralin, especially at 254 nm wavelength. For same peak heights, the mass of naphthalene is only about one twentieth of tetralin. The seneitivity to UV response at 254 nm makes small changes in quantity of naphthalene readily detectable. The peak height ratios of naphthalene to tetralin and 1-methyl-indan to tetralin have been adopted as parameters for measuring the conversion of tetralin to naphthalene and 1-methyl-indan.

These two ratios are proportional to the mass ratios of naphthalene to tetralin and 1-methyl-indan to tetralin, according to Beer's absorption law. Due to the fact that the maximum conversion of tetralin at the conditions studied in this work is 15%[16], and the tetralin used in reactions is five times that of the starting A, tetralin can be considered as the major component in the reaction products. The concerntrations of A in all the PS + T fractions are nearly constant. Therefore, the A fraction can be used as a internal reference and the peak height ratio can be used as a parameter for measuring the conversion of tetralin without much deviation, especially for qualitative comparison. One main advantage of this method is the elimination of any possible loss during the preparation of samples, which is a very serious problem when the mass or concentration is obtained by comparing the peak height or peak area with a calibration curve.

The C_{18} chromatogram peak height ratios of naphthalene to tetralin of PS +T fractions from three isothermal runs, shown in Tables XXV to XXVII, are plotted vs. reaction time in Figure 20. For comparison, the results from Run. No.22 are also plotted, of which reaction conditions are the same as isothermal run at 760°F. The only difference is that in Run No. 22 tetralin without the A was heated from room temperature to 760°F and kept isothermally at that temperature for 20 hours. It is clear that the formation of naphthalene from tetralin is enhanced in the presence of asphaltene. It also shows that the rate of formation of naphthaltene in the presence of asphaltene changes abruptly at two different stages. In contrast, the formation of naphthalene vs.time in Run No. 22 is a very smooth curve. It seems that there is a exceptional case at 820°F. However, when the C_{18} chromatogram peak height ratios of 1-methyl-indan to tetralin of PS + T fractions from 820° F isothermal run are plotted vs. reaction time in comparison with those from Run No. 40 in Figure21 , the observation of stages is also shown quite distinctly. One logical reason is that 1-methyl-indan is the major product from tetralin at 820°F.

The time that the rate of naphthalene formation changes abruptly is around 2 and 4 hours for 705°F isothermal reaction run, 1 and 2 hours for 760°F, and 0.75 and 2.0 hours for 820°F. The time found here corresponds to the time (t_1 and t_2) reported from kinetic conversion. Those are two absolutely independent studies. The results obtained here can serve as experimental evidence for the kinetic model developed in this study.

4. Chemical Structure and Composition of Products

The ultimate analysis of Table XII shows that the BI fraction contains 31.58% ash. It was suspected that this fraction probably contained some of the unreacted coal. Therefore, this

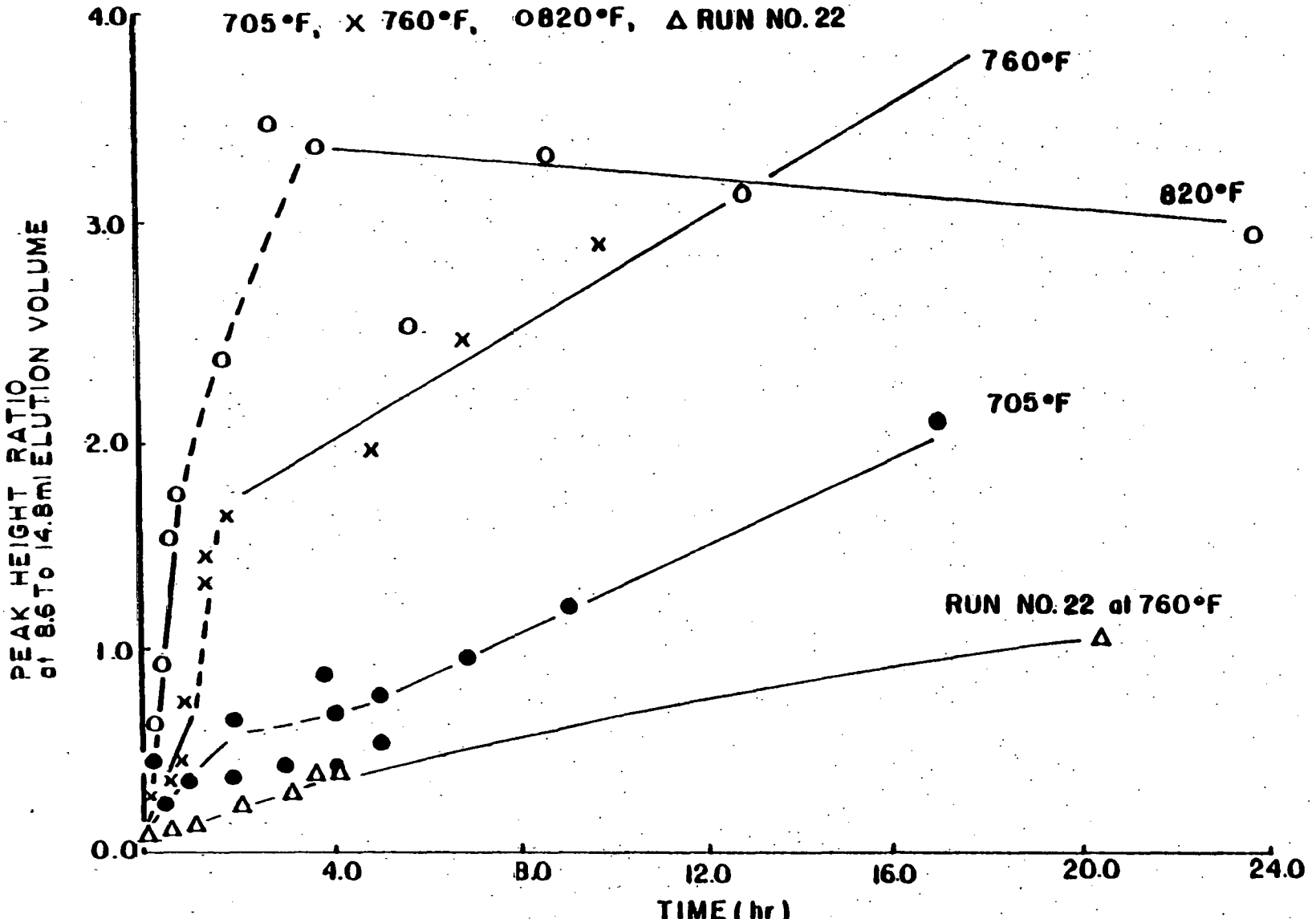

Figure 20. C_{18} Chrcmatogram Peak Height Ratio at 8.6 to 14.8 ml Elution Volume vs. Reaction Time

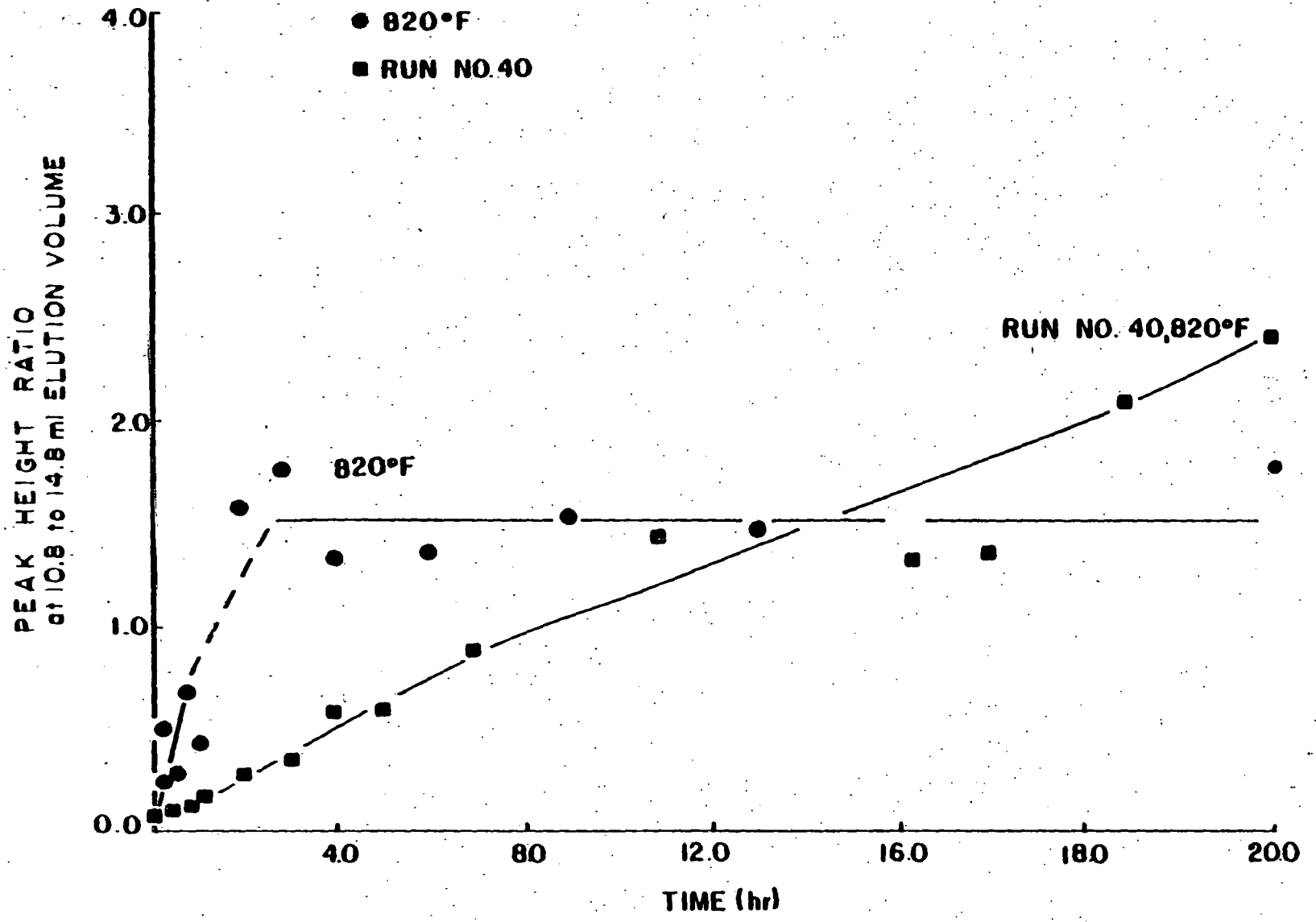

Figure 21. C_{18} Chromatogram Peak Height Ratio at 10.8 to 14.8 ml Elution Volume vs. Reaction Time

fraction was Soxhlet-extracted with THF to obtain a THF soluble fraction(TS) and a THF insoluble fraction (TI). The elemental analysis of these two fractions are also shown in Table XII. In terms of these four fractions, this SRC II stripper bottom product contains 47.2%, of PS, 18.5% of A, 6.6% of TS, and 27.2% of TI which is unconverted coal and unreactive ash. The BI fraction obtained in the isothermal reactions are all soluble in the THF and should belong to the TS fraction.

It may be seen from Table XII that heteroatoms and ash are generally concentrated in the A, TS, and TI fractions, and the atomic H/C ratios decrease in going from PS to A to TS and to TI. This is in agreement with the results observed with other investigators. [1]

The carbon, hydrogen, and heteroatom contents of A5 in Table XII, together with those of other asphaltenes after isothermal reaction, shown in Tables XIII to XV, and quite similar to the starting asphaltene. However, the atomic H/C ratios of those asphaltenes after reaction are always lower than that of the starting asphaltene. It seems that this ratio decreases as conversion increases for a isothermal run, although the data are somewhat scattered.

The molecular weight results shown in Tables XVI to XIX indicate that association of the PS, A, and the asphaltenes after reaction takes place in benzene over the concentration range of 4-30 g/l. All of the samples afford positive linear correlations between concentration and molecular weight. The correlation coefficients of 22 of the 26 least-squares equations in benzene are greater than 0.97. This means that the assumption [2-4] that molecular weights vs. concentration may be reasonably approximate as linear in dilute solution is also valid in this study. The molecular weight values obtained by extrapolating to infinite dilution approximate the true, unassociated monomer molecular weights and are used in this study. The slope of the molecular weight vs. concentration curve can be used as the measure of association. For the A fraction, the slope of the linear correlation line in benzene is greater than that in THF, but the molecular weight values obtained at infinite dilution are in good agreement. This suggests that association is more significant in the less polar solvent benzene, but dissociation tends to go to completion in either solvent at infinite dilution. Since the variation of molecular weights at infinite dilution in benzene and THF is 0.2% for PS, and 5.0% for A, it is safe to determine the molecular weight in benzene solvent only. Therefore, the molecular weight (MW) used in this study means the molecular weight obtained by extrapolating to infinite dilution in solvent benzene, unless otherwise specified.

The MW of PS is 193.0 while that of A is 358. These two values are average MW at infinite dilution in benzene and THF. The A16 formed from pyrolyzing PS without tetralin has almost the same MW (354.2) as A(358). The molecular weights of the remianing asphaltenes after reaction become larger than the starting asphaltene (A). For an isothermal run, the molecular weights of asphaltenes increase as reaction

continues. The fact that the slopes of the linear correlation lines increase in the same order, suggests that association follows the same trend as size. This seems to indicate that the smaller molecules are first preferentially converted to PS and BI, and the larger molecules are concentrated in the remaining asphaltene, which shows stronger association than before in the solvent benzene. However, the molecular weights of A 38-4 and A 38-7 become small, which suggests that the asphaltenes begin to crack into smaller molecules since the temperature is quite high (820°F) and the reaction time is long (9.0 & 24 hr).

By the modified Brown-Ladner Equations (Table I) from the proton NMR data in combination with elemental analysis and MW, the average properties of PS, A, A5 and asphaltenes from isothermal reactions were calculated and are presented in Tables XX to XXIV. The PS is a fairly aromatic species. It has approximately 74% of the carbon as aromatic carbon and two aromatic rings per average molecule. Eighty-six percent of total aromatic atoms are substitutable aromatic edge atoms, of which 27% are substituted. The average number of carbon atoms per saturatdd substitutent ranges about 1.5.

The A molecule is highly aromatic,having around 82% of the carbon as aromatic carbon. The number of aromatic rings ranges about 4.8 per average molecule. Sixty-six percent of total aromatic atoms are substitutable aromatic edge atoms, of which 24% are substituted. The average number of carbon atoms per saturated substituent is 1.7.

The high aromaticities and aromatic ring sizes, and low substituents of PS and A suggest that this SRC-II is a mild process for coal liquefaction in which coal and coal liquefaction intermediates have been converted to small molecules in a smaller degree than in other types of processes, like H-Coal and EDS. Another possible reason is that this product is stripper bottoms, and has had a high percentage of saturated molecules removed in the stripper.

The NMR proton percentages show a definite increase in the percentage of aromatic protons for all the asphaltenes remaining after reaction. The values of f_a, H_{aru}/C_{ar} and C_A also increase for most of the asphaltenes remaining after reaction. These results indicate that the asphaltene remaining has more aromatic carbon atoms and becomes more aromtic than the starting A. The newly converted aromatic carbons are substitutable edge atoms. Those hydrogen released by this aromatization could stabilize part of the free radicals produced by thermal degradation of low molecular weight asphaltenes, and result in the formation of the PS fraction. This tends to support the hydrogen shuttling mechanism proposed by Whitehurst et al.[17]

Since the A starts to crack when the temperature is 820°F and the reaction time is longer than 9.0 hour, the number of aromatic carbon atoms of A 38-4 and A 38-7 decrease. This observation is in agreement with that of the decrease

of MW of those two asphaltenes. The cracked molecules are highly aromatic species which contain more condensed aromatic ring systems, since they have higher f_a and less H_{aru}/C_{ar} values.

Infrared analysis has been used qualitatively to determine certian functional groups and to compare the samples for similarities or differences over the 600-4000 cm^{-1} region. IR spectra of PS and PS formed from isothermal reaction of A are generally very similar. All of them have strong phenolic OH absorption at 3600 cm^{-1}, pyrolic NH absorption at 3470 cm^{-1}, asymmetric and symmetric CH stretching at 2925 cm^{-1} to 2860 cm^{-1}, and C=C stretching at 1600 cm^{-1}. The main differences of IR spectra between PS and PS from reaction are at 1235 cm^{-1} and 800 cm^{-1}. The former is assigned to C-O stretching while the latter to aromatic out of plane C-H bending. All of PS formed from reaction have stronger absorption at those two wavenumbers than the PS without reaction. This is not very surprising since the PS formed is from conversion of A which is a highly aromatic species.

Gel permeation chromatography (GPC) uses column packed with swelled polymer particles with controlled pore size. Molecules are separated through GPC column according to molecular size based upon a distribution between a stationary phase of controlled pore size distribution and mobile liquid phase. Larger molecules elute faster than smaller molecules since larger molecules have lower probablities of diffusion into the liquid trapped inside the pore. The GPC chromatograms of asphaltene in Figure10 show that the starting A has two peaks at elution volumes of 23 ml and 26 ml. Small molecules corresponding to the peak at 26 ml disappear after reaction and are converted to pentane soluble fractions. Larger molecules corresponding to the peak at 23 ml still remain as asphaltenes which are shown in Figure10 as A3, A13-3, and A5. This observation is in very good agreement with that from molecular weight determination, which suggests that smaller molecules are first preferentially converted to PS and BI, and the larger molecules are concentrated in the reamining asphaltenes.

The GPC chromatograms of those pentane soluble products converted from A shown in comparison with that of PS without reaction in Figure 11 indicate that molecular weight distributions of those samples are quite similar. The sharp peaks at an elution volume of 27 ml represent tetralin for PS+T 3, PS+T 13-3, and PS+T 5. These samples are very complex mixtures and contain many of different compounds which can not be separated by the GPC column. Therefore, a reverse phase Micro-bondapak C_{18} column replaced those GPC columns for studying all the PS+T fractions produced from isothermal reactions. The result obtained by use of this column tends to support the kinetic model proposed in this study, which has been disscussed in the last section (6.3).

It has been observed in the previous section that naphthalene and 1-methyl-indan have been formed from tetralin during the reaction studied. The mechanism of conversion of tetralin to these two compounds involves the releasing or transferring of hydrogen free radicals.[16] These hydrogen free radicals can stabilize part of the asphaltene free radicals produced by thermal degradation of low molecular weight asphaltenes or serve as hydrogen transferring mediums in the hydrogen shuttling mechanism. In both cases, the pentane soluble fractions are formed. At 705° or 760°F, these hydrogen free radicals produced react mainly with the asphaltene to form the PS. At 820° F, however, the hydrogen free radicals produced are more than enough. Some of them start to attack the solvent tetralin and form 1-methyl-indan. When the reaction time is long, they go back to stabilize the asphaltene free radicals produced by cracking of the large molecules remaining. Therefore, the formation of 1-methyl-indan in Figure21 is leveling off when the reaction time is long.

5. Implications of Results

The SRC II stripper bottom product is a rather heavy material, which contains 27.7% unreacted coal and ash. The converted product is composed of 65.3% pentane soluble fraction, 25.6% asphaltene, and 9.1% benzene-insoluble but THF soluble fraction. The ash and heteroatoms such as nitrogen, sulfur, and oxygen are generally concentrated in the latter two fractions, while the atomic H/C ratios decrease in going from PS to A to TS and to TI. The MW of A is larger than the MW of PS, and the self-association of A is also stronger than that of PS in benzene solvent. In addition, the A contains more aromatic carbons, larger aromatic sheet sizes, but lower aromatic substituents than the PS. Those are consistent with results obtained by other investigators.[1,2-4,5]

A modified solvent fractionation method has been used to separate the coal liquid received. This method is simple and reproducible in high yield. This becomes the standard method used in this study to separate the coal liquid as well as the reaction products.

An autoclave reactor system equipped with automatic temperature controller, and injection loading and withdrawal systems for introducting and removing samples without disturbing the reaction, was designed and used in kinetic study. It provides high mass recovery and accurate temperature control (2.2% in temperature readout, 5% in constant temperature control). It is a system that can furnish a very close isothermal temperature profile, and give excellent definition of reaction time.

The kinetic study has revealed the kinetic scheme for

interconversion among those three fractions, which has the following form with four first order rate constants:

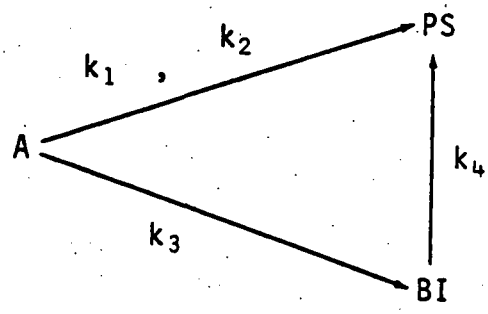

This is an overall scheme, which can actually be divided into three stages separated by time t_1 and t_2. The values of those four rate constants are obtained from experimental data at 705°, 760°, and 820°F. They show large temperature dependency, and follow Arrhenius dependency. They are given as:

$$k_1 = 1.50 \cdot 10^3 \exp\{-11{,}000/(R \cdot temp)\}$$
$$k_2 = 7.51 \cdot 10^{-1} \exp\{-3{,}700/(R \cdot temp)\}$$
$$k_3 = 1.20 \cdot 10^4 \exp\{-15{,}600/(R \cdot temp)\}$$
$$k_4 = 1.70 \cdot 10^4 \exp\{-14{,}900/(R \cdot temp)\}$$

where all rate constant are in hr^{-1}, R is ideal gas constant in cal/(g-mole · °K) and temp is temperature in °K. Since the large variations in obtaining the above values, the data presented are considered semi-quantitative. However, the present variations are much lower than those from other studies.[12-15]

Based on this kinetic scheme, the calculated values for the conversion of A to PS and BI agree well with the experimental data for all three temperatures.

This is the first time that the interconversion of coal-derived products has been studied quite thoroughly in kinetic experiment in conjunction with chemical characterization. Also, this is the first time that attempts were made in modeling of this interconversion. In addition, the secondary reaction of A to PS at third stage has never been studied before by any investigator.

It has been reported that in SRC II runs the liquid and gas yield has increased because of the recycle of reactor effluent slurry instead of distillate solvent. The increase of liquid yield, according to the model developed here, should be attributed to the secondary reaction of A to PS, as well as the conversion of BI to PS during the recycle period.

It is very clear from the kinetic scheme that the A is converted into PS via a much faster route than to BI in the first stage of the reaction. During the second stage, this fast reaction is negligible, but the formation of BI continues. The conversion of BI directly to PS starts in the meantime. When the residence time is long enough, the remaining A starts to crack, again. This is the beginning of the third stage, which the conversion of BI to PS still takes place.

The time (t_1 and t_2) that separates those three stages varies with the reaction temperature. However, it is known that a process does not have optimum conditions if the reaction residence time fall into the second stage. Shortening the reaction time within the first stage or recycling of heavy components like in SRC II is therefore recommended.

The values of t_1 and t_2 obtained from the kinetic study are very close to those derived from the HPLC study of PS+T fractions through the use of C_{18} column. The latter information tends to support the kinetic scheme developed.

When naphthalene is formed from tetralin, hydrogen free radicals are released, and then consumed. The formation of naphthalene corresponds to the hydrogen consumption, therefore. The slopes in Figures 20 represents the rate of formation of naphthalene, and hence can be used as an indication of hydrogen consumption. It is clear from the slope in Figure 20 that the hydrogen consumption rate is very fast in the first stage of the reaction at 705° and 760° F. When the reaction temperature is raised to 820°F, the fast rate is carried over to the second stage of the reaction, in which the formation of PS is low and the hydrogen is mainly used up for the production of the side product from the tetralin. This side reaction is undesirable, and can be avoided by shortening the reaction time within the first stage or switching to a lower reaction temperature.

More explicitly, the above discussion implies that a superior coal liquefaction is a process with moderate reaction temperature, short residence time, and recycle of heavy fractions in the reactor effluent, because the second stage of the reaction could be avoided or minimized in this process. The consumption of hydrogen and the cost for reactor at lower temperature could be reduced, also. In addition, much energy could be saved because of the low operation temperature and the reduction of unnecessary side reactions.

The product, the pentane soluble fraction, produced from asphaltene and, the original PS fraction are very complicate materials [18] and contain very similar functional groups as revealed in IR spectra. The main differences are that the PS fraction formed from reaction is more aromatic and contains more ether type oxygen than the PS without reaciton.

Comparing the chemical structures and compositions of the starting A with those of the asphaltenes remaining after reactions, the results obtained from various analyses are consistent with each other. The results indicate that the asphaltenes with small molecules are first preferentially converted, and the asphaltenes with large molecules are concentrated in the remaining asphaltenes. Those remaining asphaltenes have lower atomic H/C ratio, stronger self-association in benzene, and higher aromaticity than the starting A. This tends to support the hydrogen shuttling

mechanism. It is not necessary that the hydrogen shuttling and thermal degradation happen on same molecule. It is possible that the hydrogen released from one asphaltene molecule could stabilize the free radicals produced from thermal degradation of other asphaltene molecules. The former asphaltene becomes more aromatic and remains insoluble in pentane. The stabilized molecules are soluble in pentane because of the staturation, and smaller molecular size. However, this does not mean that the hydrogen donor transfer mechanism is excluded, since the aromaticity increase of the remaining asphaltene is not that much, nor is the hydrogen released based on the hydrogen shuttling mechanism.

The hydrogen donor transfer mechanism is supported by the HPLC study using C_{18} column. The tetralin is hydrogen donor, while the asphaltene is the acceptor. In the presence of the acceptor, the formation of naphthalene from tetralin is enhanced, during which hydrogen free radicals are released and consumed.

References

1. Schwager, I., and Yen, T.F., "Coal-Liquefaction Products from Major Demonstration Processes. 1. Seperation and Analysis," Fuel, 57, 100 (1978).

2. Schwager, I., Lee, W.C., and Yen, T.F., "Molecular Weight and Association of Coal-Derived Asphaltenes," Anal. Chem., 49, 2363 (1977).

3. Lee, W.C., Schwager, I., and Yen, T.F.,"Novel Approaches for Determination of Degree of Association of Coal-Derived Products by Vapor Pressure Osmometry," ACS Div. Fuel Chem., Preprints, 23(2), 37 (1978).

4. Yen, T.F., et al., "Chemistry and Structure of Coal-Derived Asphaltenes and Preasphaltenes," DOE Report No. FE-2030-14, N.T.I.S. (1979).

5. Schwager, I., Farmanian, P.A., and Yen, T.F.,"Structural Characterization of Solvent Franctions from Five Major Coal Liquids by Proton Nuclear Magnetic Resonance," Analytical Chemistry of Liquid Fuel Sources, P.C. Uden, S. Siggia, and H.B. Jensen, Ed., American Chemical Society, Washington, D.C.(1978).

6. Friedel, R.A., and Retcofsky, H.L.,"Spectrometry of Chars-Structure Studies," Spectrometry of Fuels, R.A. Friedel, Ed., Plenum Press, New York (1970).

7. Schwager, I., and Yen, T.F., "Determination of Nitrogen and Oxygen Functional Groups in Coal-Derived Asphaltenes," Anal. Chem., 51, 569 (1979).

8. Weller, S., Pelipetz, M.G., and Friedman, A., "Kinetics of Coal Hydrogenation-Conversion of Asphalt," Ind. & Eng. Chem., 43. 1572 (1951).

9. Weller, S., Pelipetz, M.G., and Friedman, S., "Kinetics of Coal Hydrogenation-Conversion of Anthraxylon," Ind. & Eng. Chem., 43, 1575 (1951).

10. Curran, G.P., Struck, R.T., and Gorin, E., "Mechanism of the Hydrogen-Transfer Process to Coal and Coal Extract," Ind.& Eng. Chem., Process Des. Dev., 6,166 (1967).

11. Yoshida, R., Maekawa, Y., Ishii, T., and Takeya, G., "Mechanism of High-Pressure Hydrogenalysis of Hokkaido Coal (Japan). 1. Simulation of Product Distributions," Fuel, 55, 337 (1976).

12. Han, K.W., Dixit, V.B., and Wen, C.Y.,"Analysis and Scale-up Consideration of Bituminous Coal Liquefaction Rate Processes," Ind. & Eng. Chem., Process Des. Dev., 17,16 (1978).

13. Brunson, R.J., "Kinetics of Donor-Vehicle Coal Liquefaction in a Flow Reactor," Fuel, 58,203 (1979)

14. Cronaur, D.C., Shah, Y.T., and Ruberto, R.G.,"Kinetics of Thermal Liquefaction of Belle Ayr Subbituminous Coal," Ind. & Eng. Chem., Process Des. Dev., 17, 281 (1978).

15. Shalabi, M.A., Baldwin, R.M., Bain, R.L., Gary, J.H., and Golden,J.O., "Noncatalytic Coal Liquefaction in a Donor Solvent. Rate of Formation of Oil, Asphaltenes, and Preasphaltenes," Ind. & Eng. Chem., Process Des. Dev., 18, 474 (1979).

16. Hooper, R.J., Battaerd, H.A.J., and Evans, D.G., "Thermal Dissociation of Tetralin between 300 and 450° C," Fuel, 58, 132 (1979).

17. Whitehurst, D.D., Farcasiu, M., Mitchell, T.D., and Dickert, J.J.,"The Nature and Origen of Asphaltness in Processed Coals," EPRI Report No. AF-480 (July, 1977).

18. Aczel, T., Williams, R.B., Brown, R.A., and Pancirov, R.J., "Chemical Characterization of Synthoil Feeds and Products," Analytical Methods for Coal and Coal Products, Vol. I,C. Karr, Jr., Ed., Academic Press, N.Y., N.Y. (1978).

```
C     PROGRAM 1
C
C
C
C     DETERMINATION OF MOLECULAR WEIGHT BY VAPOR PRESSURE OSMOMETER
C     CALIBRATION CURVE
      DIMENSION T(40),CM(40),T1(40),X(40),Y(40),SCM(40)
 201  FORMAT (I2)
      READ (1,201)NC
      READ (1,202) (T(I1),CM(I1),I1=1,NC)
 202  FORMAT (2F10.5)
      SUMCM=0.0
      SUMT=0.0
      SMCM2=0.0
      SMCMT=0.0
      SMIT=0.0
      DO 203 J1=1,NC
      SUMCM=SUMCM+CM(J1)
      SUMT=SUMT+T(J1)
      SMCM2=SMCM2+CM(J1)**2
      SMCMT=SMCMT+CM(J1)*T(J1)
      SMIT=SMIT+T(J1)*T(J1)
 203  CONTINUE
      A1=SMCMT/SMCM2
C     THE EQ. FO CALIBRATION CURVE IS   T(I)=A1*CM(I)
      WRITE(21,204)NC
 204  FORMAT ('1','CALIBRATION CURVE'/'  NUMBER OF DATA POINS = ',I2//
     110X,'T',14X,'M')
      WRITE(21,205)(T(K1),CM(K1),K1=1,NC)
 205  FORMAT (2F15.5)
      WRITE(21,206) A1
 206  FORMAT('  THE EQ. IS   T(I) = ',F11.5,' M(I)')
C     CALCULATION OF MOLECULAR WEIGHT OF SAMPLE USING CALIBRATION CURVE
 101  READ(1,103) N
 103  FORMAT (I2)
```

```
      IF(N.EQ.0) GO TO 102
      READ(1,104)(T1(I),X(I),I=1,N)
104   FORMAT  (2F10.5)
      DO 105 T11=1,N
      SCM(I11)=T1(I11)/A1
      Y(I11)=X(I11)/SCM(I11)
105   CONTINUE
      LEASE SQUARES FIT OF STRAIGHT LINE   (Y=AX+B)
      SUMX=0.0
      SUMY=0.0
      SMXX=0.0
      SMXY=0.0
      SMYY=0.0
      DO 11 J=1,N
      SUMX=SUMX+X(J)
      SUMY+SUMY+Y(J)
      SMXX=SMXX+X(J)*X(J)
      SMXY=SMXY+X(J)*Y(J)
      SMYY+SMYY+Y(J)*Y(J)
11    CONTINUE
      G=N
      DEN=G*SMXX-SUMX*SUMX
      YEN=G*SMYY-SUMY*SUMY
      A=(G*SMXY-SUMX*SUMY)/DEN
      B=(SMXX*SUMY-SUMX*SMXY)/DEN
      D=(Y-AX-B)
      SMDD=0.0
      DO 12 J=1,N
      SMDD=SMDD+(Y(J)-A*X(J)-B)*(Y(J)-A*X(J)-B)
12    CONTINUE
      STDY=SQRT(SMDD/(G-2))
      STDB=STDY*SQRT(SMXX/DEN)
      STDA=STDY*SQRT(G/DEN)
      COCO=SQRT((G*SMXY-SUMX*SUMY)*(G*SMXY-SUMX*SUMY)/(DEN*YEN))
      WRITE(21,13)N
```

```
13    FORMAT ('1','NUMBER OF DTA POINTS = ',I2///8X,'M.W.',10X,
     1'C(GM/L)',5X,'T(V.P.O. READING)',15X,'M')
      WRITE (21,14)  (Y(K),X(K),TI(K),SCM(K),K=1,N)
14    FORMAT  (2F15.5,2F20.5)
      WRITE (21,15) A,B
15    FORMAT (///'  THE EQ. IS     M.W. = ',F10.5,' C + ',F10.5)
      WRITE (21,19) STDY,STDB,STDA,COCO
19    FORMAT (//'STDY = ',F10.5/'STDB = ',F10.5/'STDA = ',F10.5/'
     1COCO = ',F10.5)
      GO TO 101
102   STOP
      END
```

```
C        PROGRAM 2
C
C
C
C
C
C       CALCULATION OF THE STRUCTURE PARAMETERS
C       MODIFIED EQUATION (H-AR. IS SUBSTITED BY ((H-AR.) -(0.5$ )/H))
C       IT IS NOT NECESSARY TO NORMALIZE SA1P, SA2P AND SA3P IN THE
C       PROGRAM
        OPEN (UNIT = 24,FILE = "NMR.DAT")
 101    READ (24,102) WC,WH,WO,WM,N,M
 102    FORMAT (4F10.5,2I2)
        IF (WC.EQ.0.0) GO TO 103
        WRITE (22,109)
 109    FORMAT ("1",5X,"C%",6X,"H%",5X,"O%",6X,"M",4X,"H-AR.  H-BE.
       1H-SA.",6X,"FA",7X,"SEGMA",7X,"HOC",8X,"CAN",9X,"RA",8X,"ANC"//)
C       WC, WH AND WO ARE WEIGHT PER CENT OF CARBON, HYDROGEN AND
C       OXYGEN, AND WM IS THE MOLECULAR WEIGHT
        GO TO (121,122,123,124,1251),N
 121    WRITE (5,125)
        WRITE (22,125)
 125    FORMAT (1X,"FMC-COED")
        GO TO 103
 122    WRITE (5,126)
        WRITE (22,126)
 126    FORMAT (1X,"SYNTHOIL")
        GO TO 130
 123    WRITE (5,127)
        WRITE (22,127)
 127    FORMAT (1X,"PAMCO")
        GO TO 130
 124    WRITE (5,128)
        WRITE (22,128)
 128    FORMAT (1X,"CAT. INC.")
```

```
      GO TO 130
 1251 WRITE (5,1291)
      WRITE (22,1291)
 1291 FORMAT (1X,"HRI")
 130  GO TO (131,132,133,134,135,136),N
 131  WRITE (5,141)
      WRITE (22,141)
 141  FORMAT (1X,"ASPHALTENE")
      GO TO 150
 132  WRITE (5,142)
      WRITE (22,142)
 142  FORMAT (1X,"CARBOID")
      GO TO 150
 133  WRITE (5,143)
      WRITE (22,143)
 143  FORMAT (1X,"RESIN")
      GO TO 150
 134  WRITE (5,144)
      WRITE (22,144)
 144  FORMAT (1X,"OIL")
      GO TO 150
 135  WRITE (5,145)
      WRITE (22,145)
 145  FORMAT (1X, "CARBENE")
      GO TO 150
 136  WRITE (5,146)
      WRITE (22,146)
 146  FORMAT (1X,"CHROMATOGRAPHY")
 150  CONTINUE
      READ (24,104)SA1P,SA2P,SA3P
 104  FORMAT (3F10.5)
      READ (24,401)WN,WS,WA
 401  FORMAT (3F10.5)
C     WN, WS AND WA ARE WEIGHT PER CENT OF NITROGEN, SULFUR AND ASH
```

```
      WTB = 100.-WA
      PFC = WM*WC/(12.01*WTB)
      PFH = WM*WH/(1.008*WTB)
      PFN = WM*WN/(14.007*WTB)
      PFO = WM*WO/(16.0*WTB)
      PFS = WM*WS/(32.06*WTB)
      WRITE (5,402)WN,WS,WA
      WRITE (22,402)WN,WS,WA
  402 FORMAT (15X,"N%=",F10.5," S%=",F10.5," ASH%=",F10.5//)
      WRITE (5,403)
      WRITE (22,403)
  403 FORMAT (15X,"MOLECULAR FORMULA = C",6X,"H",5X,"N",5X,"O",5X,"S")
      WRITE (5,404)PFC,PFH,PFN,PFO,PFS
      WRITE (22,404)PFC,PFH,PFN,PFO,PFS
  404 FORMAT (36X,F6.2,1X,F5.2,2X,F5.2,1X,F5.2,1X,F5.2//)
      ST = 100.0
      SA1 = SA1P/ST
      SA2 = SA2P/ST
      SA3 = SA3P/ST
C     SA1 IS THE FRACTION OF THE TOTAL HYDROGEN ON AROMATIC CARBON
C    1ATOMS, SA2 ON ALPHA CARBON ATOMS AND SA3 THAT ON OTHER NON-
C    1AROMATIC CARBON ATOMS
C     FA  = FRACTION OF AROMATIC CARBONS PER MOLECULE
C     SEGMA = DEGREE OF SUBSTITION OF THE AROMATIC SYSTEMS (FRACTION
C     OF AVAILABLE ARCUATIC EDGE OF ATOMS SUBSTITUTED).
C     HOC = ATOMIC HYDROGEN TO CARBON RATIO OF THE HYPOTHETICAL
C     UNSUBSTITUTED AROMATIC MATERIAL
C     CAN = TOTAL NUMBER OF AROMATIC RING CARBONS PER MOLECULE
C     ANC = AVERAGE NUMBER OF CARBON ATOMS PER SATURATED SUBSTITUENT
C     N = 1 FMC-COED, N = 2 SYNTHOIL, N = 3 PAMCO, N = 4 CAT.INC.,
C     N = 5 HRI
C     M = 1 ASPHALTENE, M = 2 CARBOID, M = 3 RESIN, M = 4 OIL,
C     M = 5 CARBENE, M = 6 CHROMATOGRAPHY
      X12 = 1.8
```

```
      Y12 = 1.8
301   X11 = 1./X12
      Y11 = 1./Y12
      FA = (WC*1.0079/(12.011*WH)-X11*SA2-Y11*SA3)/(WC*1.0079/(12.011
     1*WH))
      SEGMA = (WO*1.0079/(WH*15.999)+X11*SA2)/(SA1+X11*SA2+(WO*1.0079/
     1(WH*15.999)))
      HOC = (SA1+X11*SA2+WO*1.0079/(WH*15.999))/(WC*1.0079/(WH*12.011)
     1-X11*SA2-Y11*SA3)
C     WCC IS THE WEIGHT PER CENT OF CARBON BASED ON ASH FREE SAMPLE
      WCC = 100.*WC/(100.-WA)
      CAN = FA*WCC*WM/1200.
      RS = SEGMA*CAN*HOC
      RA = CAN*(1.-HOC)/2.+1.
      ANC = SA3P/SA2P+1.
      WRITE (5,202)X12,Y12
      WRITE (22,202)X12,Y12
202   FORMAT (20X,"X=",F10.5,"Y=",F10.5//)
      WRITE (5,200)WC,WH,WO,WM,SA1P,SA2P,SA3P,FA SEGMA,HOC,CAN,RS,RA,
     1ANC
      WRITE (22,200)WC,WH,WO,WM,SA1P,SA2P,SA3P,FA,SEGMA,HOC,CAN,RS,RA,
     1ANC
200   FORMAT (4X,F5.2,2X,F5.2,2X,F5.2,2X,F6.1,2X,F5.1,2X,F5.1,2X,F5.1,
     17F11.4///)
      X12 = X12+0.10
      Y12 = Y12+0.10
      IF (Y12.LE.2.2) GO TO 301
      GO TO 101
103   STOP
      END
```

```
C       PROGRAM 3
C
C
C
C
C
C
C       LEAST SQUARES FIT OF STRAIGHT LINE   (Y = AX+B)
C       M   :NUMBER OF DATA SET
C       N   :NUMBER OF POINTS IN ONE SET OF DATA
        DIMENSION X(40),Y(40)
        NM=1
        OPEN (UNIT=22,FILE='TEST.DAT')
        READ (22,101)M
 101    FORMAT(I2)
 001    IF (NM.GT.M) GO TO 100
        READ(22,102)N
 102    FORMAT(I2)
        READ(22,103) (X(I),Y(I),I=1,N)
 103    FORMAT(2F15.7)
        SUMX=0.0
        SUMY=0.0
        SMXX=0.0
        SMYY=0.0
        SMXY=0.0
        DO 11  J=1,N
        SUMX=SUMX+X(J)
        SUMY=SUMY+Y(J)
        SMXX=SMXX+X(J)*X(J)
        SMXY=SMXY+X(J)*Y(J)
        SMYY=SMYY=Y(J)*Y(J)
 11     CONTINUE
        G=N
        DEN=G*SMXX-SUMX*SUMX
        YEN=G*SMYY-SUMY*SUMY
```

```
      A=(G*SMXY-SUMX*SUMY)/DEN
      B=(SMXX*SUMY-SUMX*SMXY)/DEN
C     D=(Y-AX-B)
      SMDD=0.0
      DO 12 J=1,N
      SMDD=SMDD+(Y(J)-A*X(J)-B)*(Y(J)-A*X(J)-B)
 12   CONTINUE
      STDY=SQRT(SMDD/(G-2))
      STDB=STDY*SQRT(SMXX/DEN)
      STDA=STDY*SQRT(G/DEN)
      COCO=SQRT((G*SMXY-SUMX*SUMY)*(G*SMXY-SUMX*SUMY)/(DEN*YEN))
      WRITE(5,13)N
      WRITE(23,13)N
 13   FORMAT('1','NUMBER OF DATA POINTS= ',I2//10X,'Y',15X,'X')
      WRITE(5,105) (Y(K),X(K),K=1,N)
      WRITE(23,105) (Y(K),X(K),K=1,N)
 105  FORMAT(2F15.8)
      WRITE(5,106) A,B
      WRITE(23,106) A,B
 106  FORMAT(///'   THE EQ. IS  :  Y=',F16.8,'X + ',F16.8
      WRITE(5,19) STDY,STDB,STDA,COCO
      WRITE(23,19) STDY,STDB,STDA,COCO
 19   FORMAT(//' STDY = ',F19.9/' STDB = ',F19.9/' STDA = ',F19.9/' CO
     1CO = ',F19.9)
      NM=NM+1
      GO TO 001
 100  STOP
      END
```

```
C       PROGRAM 4
C
C
C       MODEL IV
C       THIS IS A PROGRAM FOR COMPUTING THE PRODUCT DISTRIBUTION AND THE
C       STANDARD DEVIATION
C       M : NUMBER OF DATA SET
C       N : NUMBER OF EXPERIMENTAL POINTS IN EACH SET
        DIMENSION ET(40),EWA(40),EWPS(40),EWBI(40),WA(40),WPS(40),WBI
       1(40),WT(40)
        NM=1
        OPEN (UNIT = 24, FILE ='MODEL 4.DAT')
        READ (24,103) M
  103   FORMAT (I2)
  001   IF (NM.GT.M) GO TO 100
        READ (24,101) N,TEMP,T1,T2,RK1,RK2,RK3,RK4
  101   FORMAT (I3,3F7.2,4F10.7)
        WRITE (5,201) TEMP,T1,T2,RK1,RK2,RK3,RK4
        WRITE (20,201)TEMP,T1,T2,RK1,RK2,RK3,RK4
  201   FORMAT (/////'REACTION TEMP. = ',F10.5/8X,'T1 = ',F10.5,8X
       1'T2= ',F10.5/4X,'<1 = ',F11.7,4X,'K2 = ',F11.7,4X,'K3 - ',F11.7
       1,4X,'K4 = ',F11.7///)
        READ (24,102) (ET(I),EWA(I),EWPS(I),EXBI(I),I=1,N)
  102   FORMAT (4F10.5)
        WAT1= 100.*EXP(-(RK1+RK3)*T1)
        WPST1=RK1*100.*(1.-EXP(-(RK1-RK3)*T1))/(RK1+RK3)
        WBIT1=RK3*100.*(1.-EXP(-(RK1+RK3)*T1))/(RK1+RK3)
        WRITE (5,202) WAT1,WPST1,WBIT1
        WRITE (20,202)WAT1,WPSTI,WBIT1
  202   FORMAT (' WA(T1) = ',F10.5,4X,'WPS(T1) = ',F10.5,4X,
       1'WBI(T2)= ',F10.5//)
        PI = RK4*WAT1/(RK4-RK3)
        PII= RK3*WAT1/(RK4-RK3)
        WAT2 = WAT1*EXP(RK3*(T1-T2))
        WPST2= WPST1-PI*(EXP(RK3*(T1-T2))-1.)-
```

```
     1        (WBIT1-PII)*(EXP(RK4*(T1-T2))-1.)
      WBIT2= PII*(EXP(RK3*(T1-T2))-EXP(RK4*(T1-T2)))
     1       +WBIT1*EXP(RK4*(T1-T2))
      WRITE ( 5,212) WAT2,WPST2,WBIT2
      WRITE (20,212) WAT2,WPST2,WBIT2
212   FORMAT ( 2X,' WA(T2) = ',F10.5, 4X,' WPS (T2) = ',F10.5,4X,
     1' WBI (T2) = ',F10.5//)
      DA = 0.0
      DPS= 0.0
      DBI= 0.0
      DO 02 I1=1,N
      IF ( ET(I1).GT.T1) GO TO 21
      WA (I1) = 100. * EXP(-(RK1+RK3)*ET(I1))
      WPS(I1) = RK1* 100.*(1.-EXP(-(RK1+RK3)*ET(I1)))/(RK1+RK3)
      WBI(I1) = RK3*100.*(1. -EXP(-(RK1+RK3)*ET(I1)))/(RK1+RK3)
      GO TO 22
21    IF ( ET(I1).GT.T2) GO TO 31
      WA (I1) = WAT1*EXP(RK3*(T1-ET(I1)))
      WPS(I1) = WPST1-PI*(EXP(RK3*(T1-ET(I1)))-1.)
     1          -(WBIT1-PII)*(EXP(RK4*(T1-ET(T1)))-1.)
      WBI(I1) = PII*(EXP(RK3*(T1-ET(I1)))-EXP(RK4*(T1-ET(I1))))
     1          +WBIT1*EXP(RK4*(T1-ET(I1)))
      GO TO 22
31    WA (I1) = WAT2 * EXP (-RK2*(ET(I1)-T2))
      WPS(I1) = WPST2+WAT2*(1.-EXP(-RK2*(ET(I1)-T2)))
     1          +WBIT2*(1.-EXP(-RK4*(ET(I1)-T2)))
      WBI(I1) = WBIT2*EXP(-RK4*(ET(I1)-T2))
22    WT (I1) = WA(I1)+WPS(I1)+WBI(I1)
      DA = (WA (I1)-EWA(I1)**2.+DA
      DPS= (WPS(I1)-EWPS))**2.+DPS
      DBI= (WBI(I1)-EWBI(I1)**2.+DBI
002   CONTINUE
      WRITE ( 5,203)
      WRITE(20,203)
```

```
203   FORMAT (' TIME',3X,'WA(EXP)',2X,'WA(CAL)',2X,'WPS(EXP)',1X,
     1'WPS(CAL)',1X,'WBI(EXP)',1X,'WBI(CAL)',1X,' WT(CAL)'////)
      WRITE( 20,204)(ET(K),EWA(K),WA(K),EWPS(K),WPS(K),
     1              EWBI(K),WBI(K),WT(K),K=1,N)
204   FORMAT (1X,F5.2,2X,F7.3,2X,F7.3,2X,F7.3,2X,F7.3,2X,F7.3,2X,F7.3
     1        ,2X,F7.3//)
      G=N
      SDA =SQRT ( DA/(G-1.))
      SDPS=SQRT (DPS/(G-1.))
      SDBI=SQRT (DBI/(G-1.))
      SDT =SQRT ((DA+DPS+DBI)/(3.*G-3.))
      WRITE ( 20,205)SDA,SDPS,SDBI,SDT
205   FORMAT ('STANDARD DEVIATION OF A = ',F10.5/'STANDARD DEVIATION
     1 OF PS = ',F10.5/'STANDARD DEVIATION OF BI = ',F10.5/' STANDARD
     1DEVIATION OF TOTAL = ',F10.5////)
      TIME =0.0
25    IF (TIME.GT.24.0) GO TO 3
      IF ( TIME.GT.T1) GO TO 23
      A=100.*EXP(-(RK1+RK3)*TIME)
      PS=RK1*100.*(1.-EXP(-(RK1+RK3)*TIME))/(RK1+RK3)
      BI RK3*100.*(1.-EXP(-(RK1+RK3)*TIME))/(RK1+RK3)
      GO TO 24
23    IF (TIME.GT.T2) GO TO 32
      A = WAT1*EXP(RK3*(T1-TIME))
      PS= WPST1-PI*(EXP(RK3*(T1-TIME))-1.)
     1    -(WBIT1-PII)*(EXP(RK4*(T1-TIME))-1.)
      BI= PII*(EXP(RK3*(T1-TIME))-EXP(RK4*(T1-TIME)))
     1    +WBIT1*EXP(RK4*(T1-TIME))
      GO TO 24
32    A = WAT2* EXP(-RK2*(TIME-T2))
      PS= WPST2+WAT2*(1.-EXP(-RK2*(TIME-T2)))+WBIT2
     1*(1.-EXP(-RK4*(TIME-T2)))
      BI=WBIT2*EXP(-RK4*(TIME-T2))
24    T = A+PS+BI
```

```
      WRITE ( 20,207) TIME,A,PS,BI,T
207   FORMAT ( /'  TIME = ',F5.2,2X,'A = ',F7.3,2X,'PS = ', F7.3,2X,
     1         'BI = ',F7.3,2X,'T = ',F7.3)
      TIME = TIME + 0.25
      GO TO 25
3     CONTINUE
      NM=NM+1
      GO TO 1
100   STOP
      END
```


*U.S. GOVERNMENT PRINTING OFFICE: 1980-740-145/1044